EXHIBIT B

Intracranial Calcifications
A Pictorial Review

R. GRECH[1], S. GRECH[2], A. MIZZI[2]

[1] Waterford Regional Hospital; Waterford, Ireland
[2] Mater Dei Hospital; Msida, Malta

Key words: calcifications, intracranial, physiologic, dystrophic, genetic, developmental, vascular, infectious, inflammatory, neoplastic, endocrine

SUMMARY – *Brain calcifications are a common radiographic finding. The pathogenesis is diverse and ranges from benign physiological calcifications to a variety of pathological disorders. Whereas certain calcifications are considered an incidental finding, their presence can sometimes be crucial in making a specific diagnosis. Several pathological conditions affecting the brain parenchyma are associated with calcifications and their recognition and location might help in narrowing the differential. Knowledge of physiological calcifications is essential to avoid misinterpretation. This review illustrates a broad spectrum of CNS disorders associated with calcifications, and tries to highlight the salient radiological findings.*

Introduction

Intracranial calcifications are a common radiographic finding. The pathogenesis is diverse and ranges from benign physiological calcifications to a variety of pathological disorders.

Certain calcifications are considered incidental findings. Knowledge of physiological calcifications is essential to avoid misinterpretation. Several pathological conditions affecting the brain parenchyma are associated with calcifications and their recognition and location might help in narrowing the differential.

This review illustrates physiological calcifications as well as a broad spectrum of CNS disorders associated with calcifications, and tries to highlight their salient radiological features.

Physiologic / Dystrophic Calcifications

Physiologic calcifications are often age-related and do not always have an underlying pathological cause [1-3]. Typical locations in the brain include the pineal gland, choroid plexus, falx cerebri, tentorium cerebelli, habenula, petroclinoid ligaments and the sagittal sinus [2] (Figure 1).

Pineal gland calcifications are very common and occur in up to two thirds of the adult population. Calcification is usually coarse and compact [4]. Size is crucial as calcifications larger than 1 cm should raise suspicion of an underlying tumour [3].

Basal ganglia calcifications are often punctate and symmetrical and are located within the globus pallidus, the head of the caudate nucleus and the putamen. Though mostly physiological, they are sometimes associated with underlying conditions, summarised in Table 1.

The choroid plexus often calcifies, with the atrial portions of the lateral ventricles being the most typical site. Atypical patterns, including exuberant calcification in the region of the glomerula, calcification extending into the bodies of the lateral ventricles and calcification of the choroid plexus in the roof of the third ventricle or in the region of the foramen of Monro, raise the suspicion of underlying pathology.

A curvilinear pattern characterises calcifications occurring in the region of habenular commisure, just anterior to the pineal body. The incidence is reported to be in the region of 15% [2].

Physiological calcifications can also be seen in the cerebellum [5], with the dendate nucleus being the most common site.

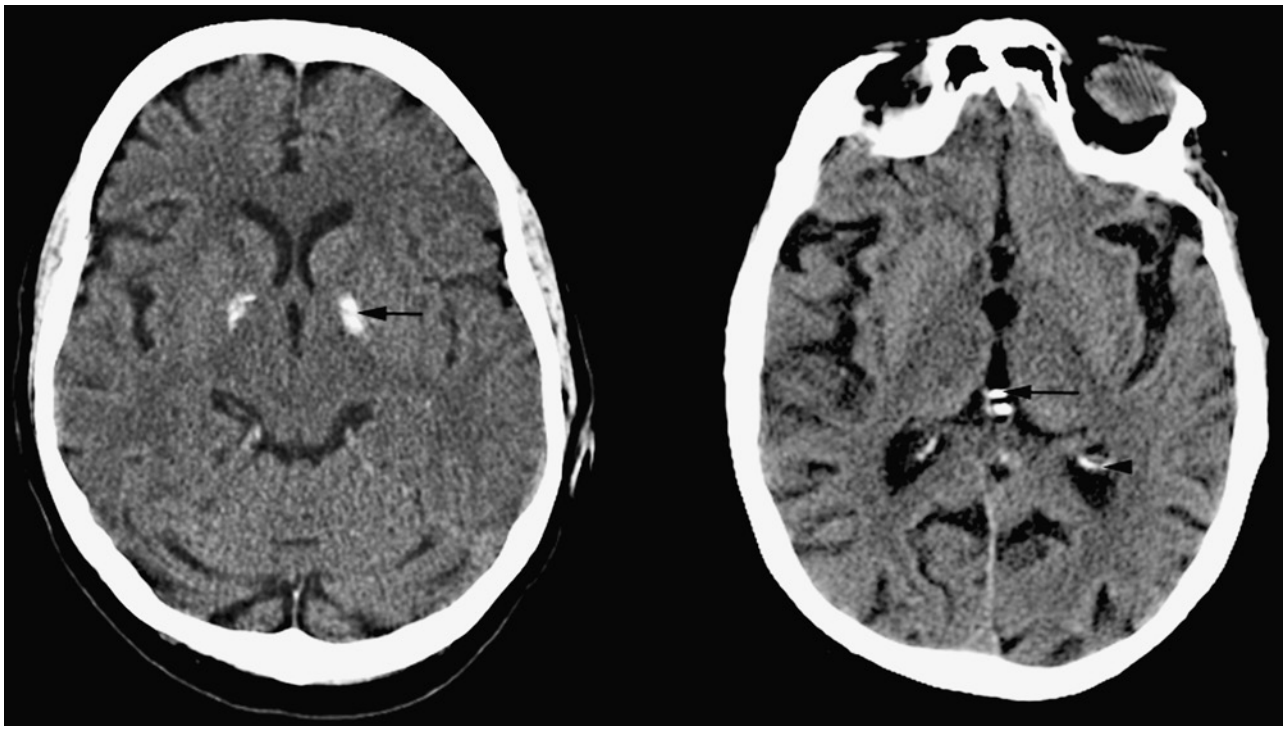

A B

Figure 1 Physiologic calcifications. A) Axial nonenhanced CT shows bilateral basal ganglia calcifications (arrow). B) CT of the same patient at the level of the thalami, shows calcifications of the pineal gland (arrow), the habenula and bilateral choroid plexuses (arrowhead).

Dystrophic calcifications are often secondary to brain insults including ischaemia, trauma and surgery [6]. They are often associated with extra axial haematomas, in particular chronic subdural haematomas (Figure 2). They are also seen as long term sequelae of radiotherapy and to a lesser extent following chemotherapy.

Genetic / Developmental Calcifications

Calcifications are a common occurrence in the neurocutaneous syndromes. They are classically described in Sturge-Weber syndrome (SWS) and tuberous sclerosis (TS) with a lower incidence in the other phakomatoses.

SWS is characterised by leptomeningeal vascular malformations. Calcification occurs in the underlying cortex and is often gyriform and curvilinear [7], sometimes appearing as parallel calcifications giving rise to the 'tram-track' sign [8] (Figure 3). The parieto-occipital cortex is mostly involved, but it may occur anywhere in the cerebrum. It can sometimes be extensive, and in 20% of patients the calcifications are bilateral.

TS is characterised by subependymal hamartomas, cortical/subcortical tubers and white matter radial migration lines (WMRMLs) [2]. Subependymal hamartomas are commonly located along the caudothalamic groove and atrium and are considered virtually pathognomonic of TS. Half of these subependymal nodules will eventually calcify (Figure 4). Cortical hamartomas are also prone to calcify. Calcifications in subependymal and cortical hamartomas are rare during the first year of life but the rate increases with the patient's age. Subependymal giant-cell astrocytomas (SEGAs), can also present as a calcified nodule [9]. Finally TS may sometimes mimic SWS when gyriform cortical calcifications are present [10].

Intracranial calcifications are also a part of the protean neurofibromatosis syndrome. The most common nontumoral calcifications described in these patients, are symmetric or asymmetric calcifications of the choroid plexus [11] in the lateral ventricles and nodular calcifications of the cerebellum [12]. Vouge et al. [13] described calcified deposits related to the ventricular walls in a series of patients with

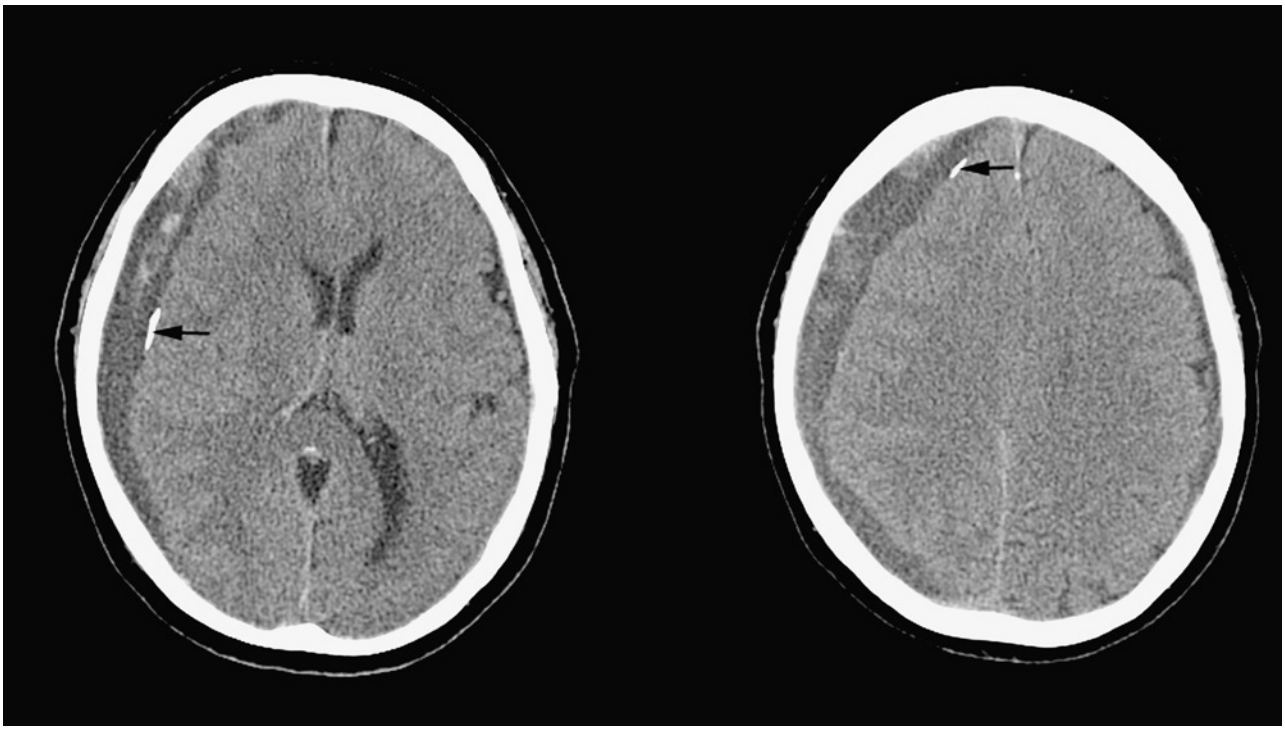

A B

Figure 2 Subdural haematoma. A, B) Axial nonenhanced CT images show acute on chronic right, subdural haematoma with calcifications (arrows) along the inner surface.

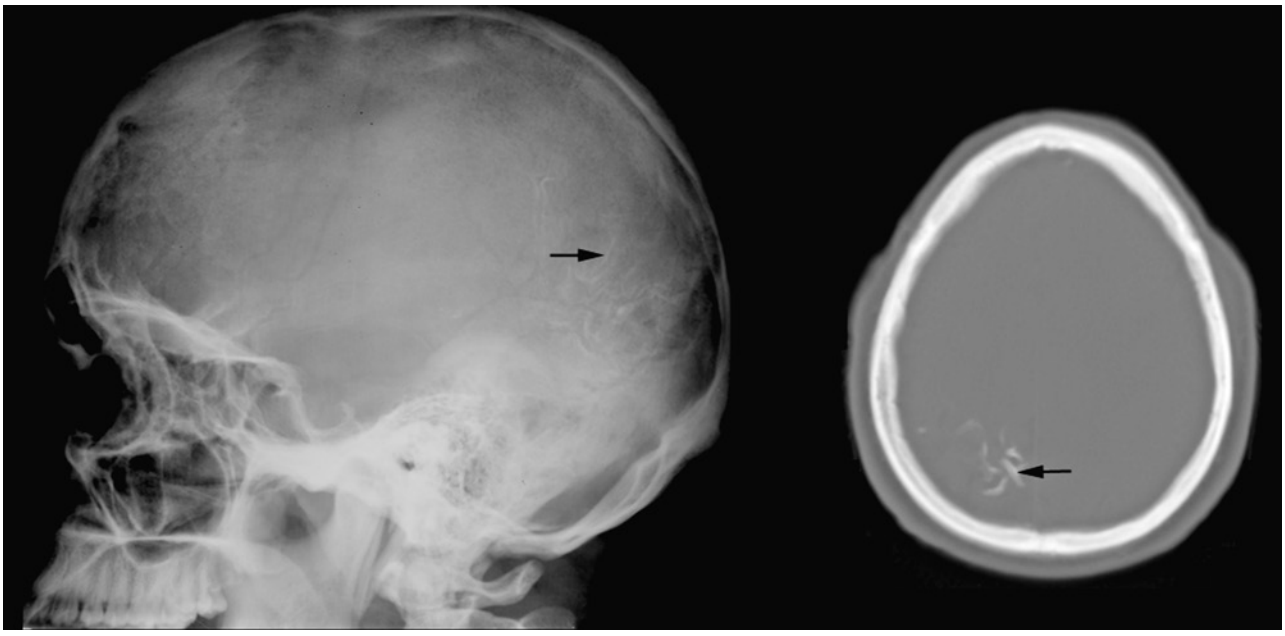

A B

Figure 3 Sturge-Weber Syndrome. A) Plain lateral radiograph of the skull demonstrates the typical tram-track calcifications (arrow) in the occipital region. B) Nonenhanced CT scan of a different patient demonstrates the linear gyral calcifications (arrow) associated with this condition.

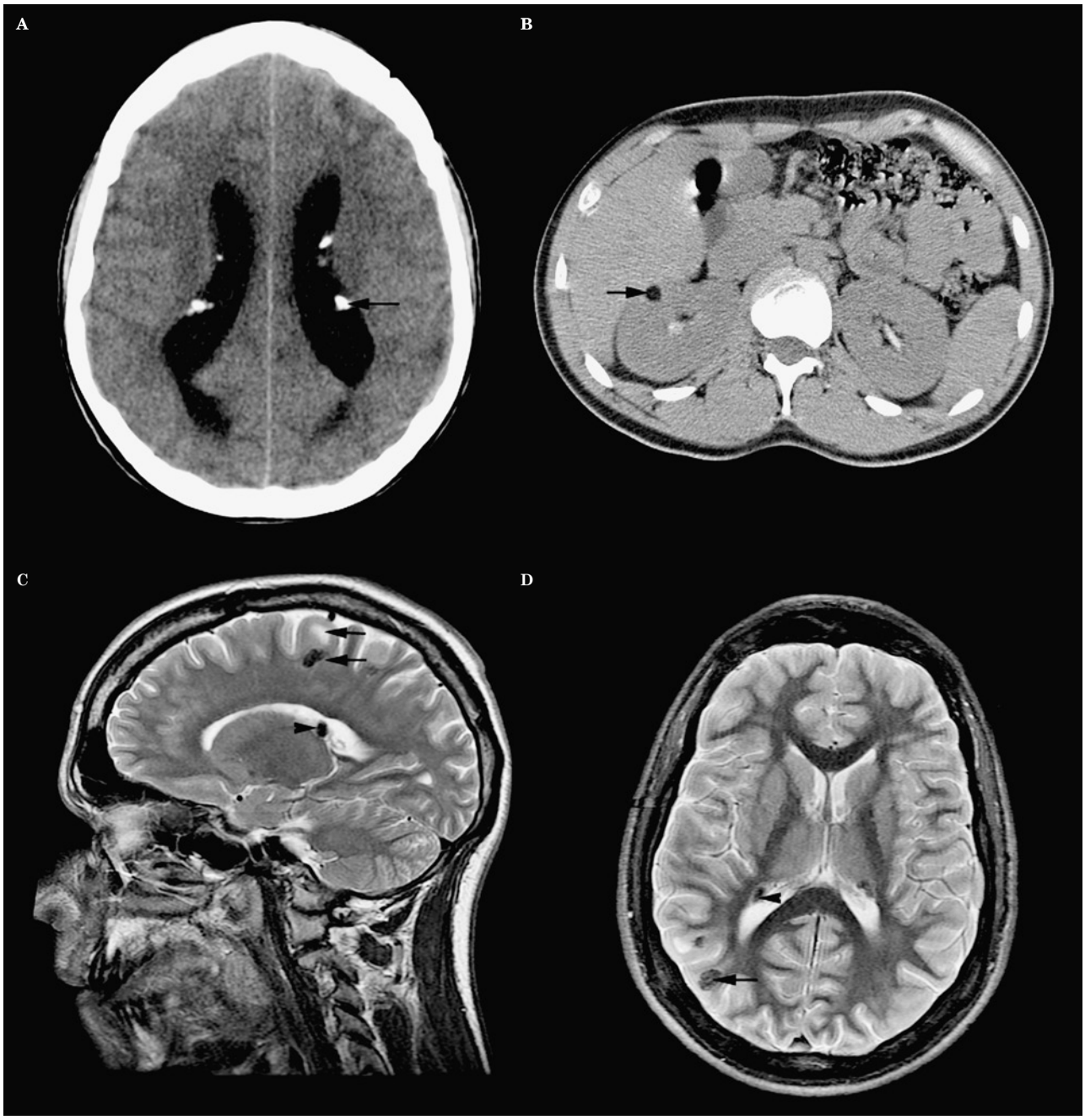

Figure 4 Tuberous sclerosis. A) Nonenhanced axial CT image shows characteristic subependymal calcifications (arrow) in both lateral ventricles. B) Abdominal CT scan demonstrates a well-defined fat containing lesion (arrow) in the right kidney, consistent with a renal angiomyolipoma. C) Sagittal T2W MR shows both high and low signal intensity white matter lesions (arrows) in the frontal lobe in keeping with subcortical tubers. A subependymal nodule (arrowhead) is also identified in the same image. D) Axial T2W MR image highlights the subcortical and subependymal tubers (arrows).

neurofibromatosis, similar to the calcifications seen in tuberous sclerosis. Basal ganglia calcifications and cortical calcifications have also been described. It is essential to differentiate between non-tumorous calcified deposits [12,14] and tumours with partial calcification. In fact the most common calcifications seen in patients with neurofibromatosis type 2 (NF2) are the ones associated with an underlying tumour, such as meningiomas [6]. The aetiology of non-

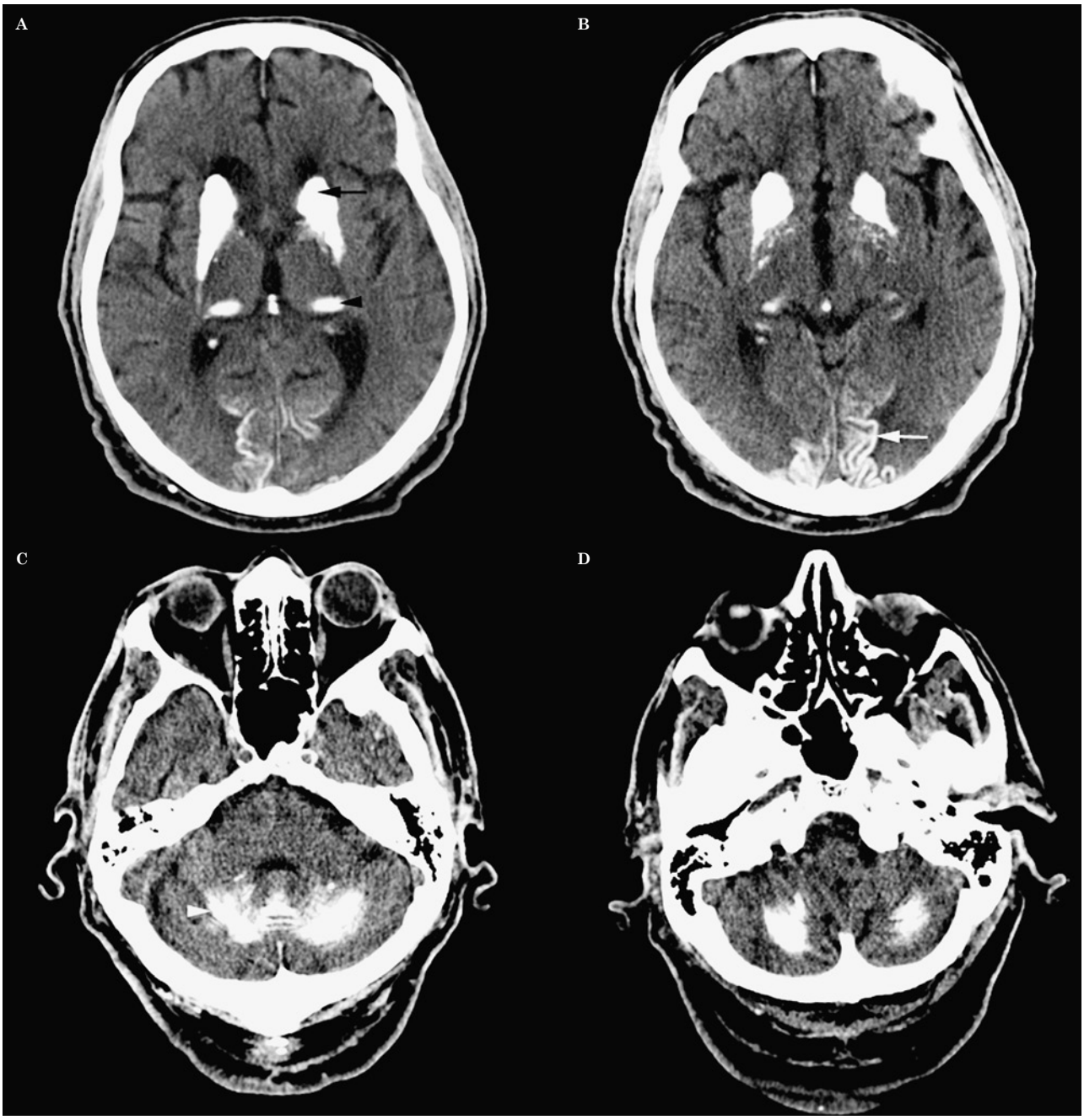

Figure 5 Fahr's disease. Extensive symmetric calcifications are seen in these nonenhanced CT images, in the regions of the basal ganglia (black arrow), the thalami (black arrowhead), and in the cerebellum with a particular predilection for the dentate nuclei (white arrowhead). Linear gyral calcifications are also seen in both occipital lobes (white arrow).

tumorous calcified deposits, is identical to that of TS and is probably caused by calcium deposition in hamartomatous glial proliferations.

Fahr's disease (FD) is a rare idiopathic neurodegenerative entity, and presents with symmetric polytopic calcifications in the basal ganglia, especially in the lateral globus pallidus. Other involved areas include the cerebral white matter, thalami, internal capsulae and the dentate nuclei of the cerebellum [15,16] (Figure 5). Cal-

Figure 6 Gorlin syndrome. A) Plain radiograph of the mandible showing two adjacent odontogenic keratocysts (arrow), associated with falx calcifications (arrowhead) in a patient with nevoid basal cell carcinoma syndrome.

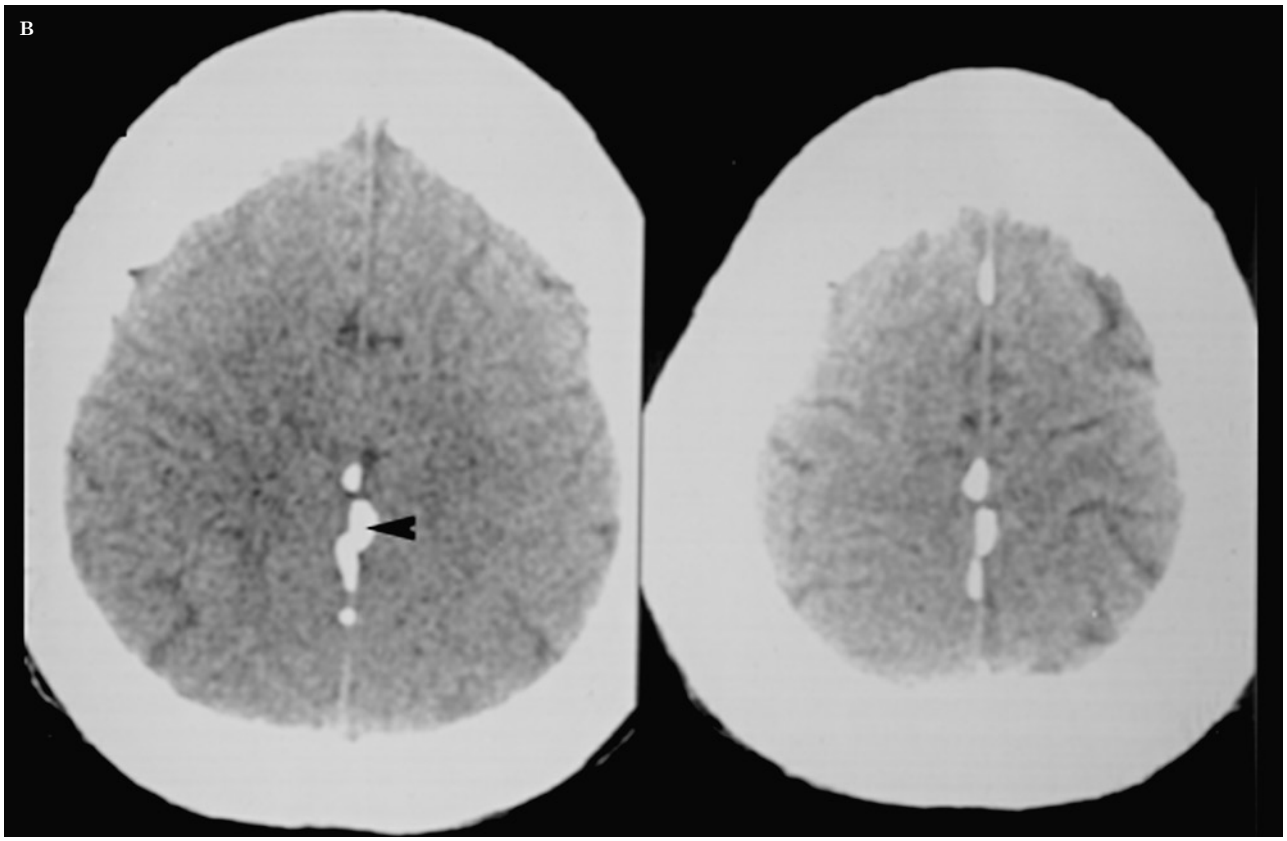

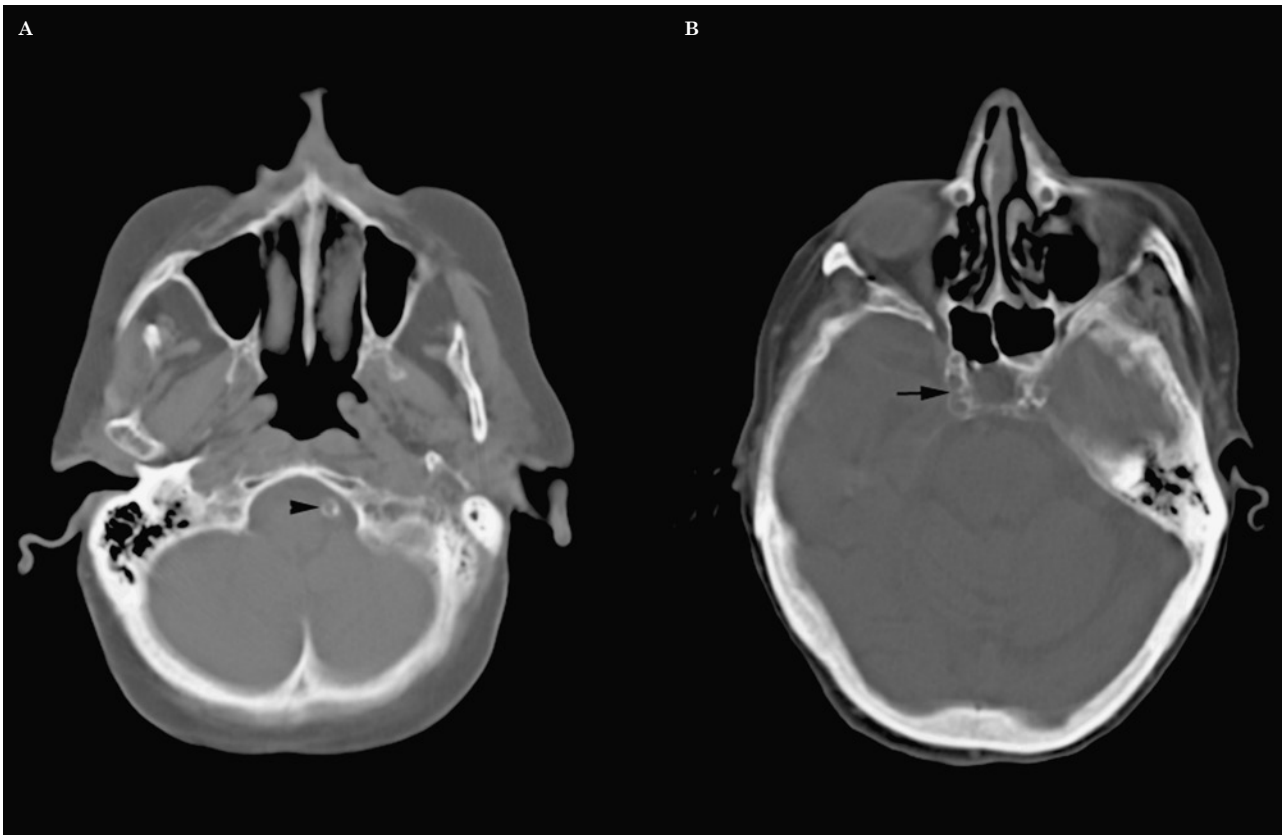

Figure 7 Vascular calcifications. Nonenhanced CT images showing prominent mural atherosclerotic calcifications in the left vertebral artery (arrowhead), and in both internal carotid arteries at the level of the carotid siphon (arrow).

cium deposits with thin linear or cloudy pattern have a high specificity, while symmetric micronodular and asymmetric unilateral calcifications are non-suggestive for FD [17]. The underlying cause is thought to be a defective iron transport mechanism resulting in tissue damage and extensive calcification. The age at onset of FD is typically the fourth or fifth decade.

Gorlin syndrome or nevoid basal cell carcinoma syndrome (NBCCS) is an autosomal dominant condition characterized by a range of developmental anomalies. Imaging findings include ectopic intracranial calcifications, odontogenic keratocysts (Figure 6), and macrocephaly.

Vascular Calcifications

Intracranial artery calcification (IAC) is frequently observed on brain computed tomography and the incidence increases with age (Figure 7). Most are mural calcifications, caused by atherosclerosis [18]. Though considered to be benign, their presence has been shown to have a predictive value for ischemic cerebrovascular events [19]. In fact the frequency of IAC is significantly higher in stroke patients than in non-stroke patients. The highest prevalence is seen in the internal carotid artery (60%) particularly in the carotid siphon segment [18], followed by the vertebral artery (20%), middle cerebral artery (5%), and basilar artery (5%) [20].

Other calcification patterns are associated with vascular pathology, such as vascular malformations and aneurysms. Brain aneurysms often have mural calcifications (Figure 8), more so in fusiform compared with saccular aneurysms. Partially or completely thrombosed aneurysms also commonly calcify [21].

Calcifications associated with arteriovenous malformations (AVM), usually occur in the walls of ectatic vessels, and occasionally extend into the surrounding gliotic parenchyma [20] (Figure 9). These appear as curvilinear streaks, or a lacelike pattern of punctuate collections on

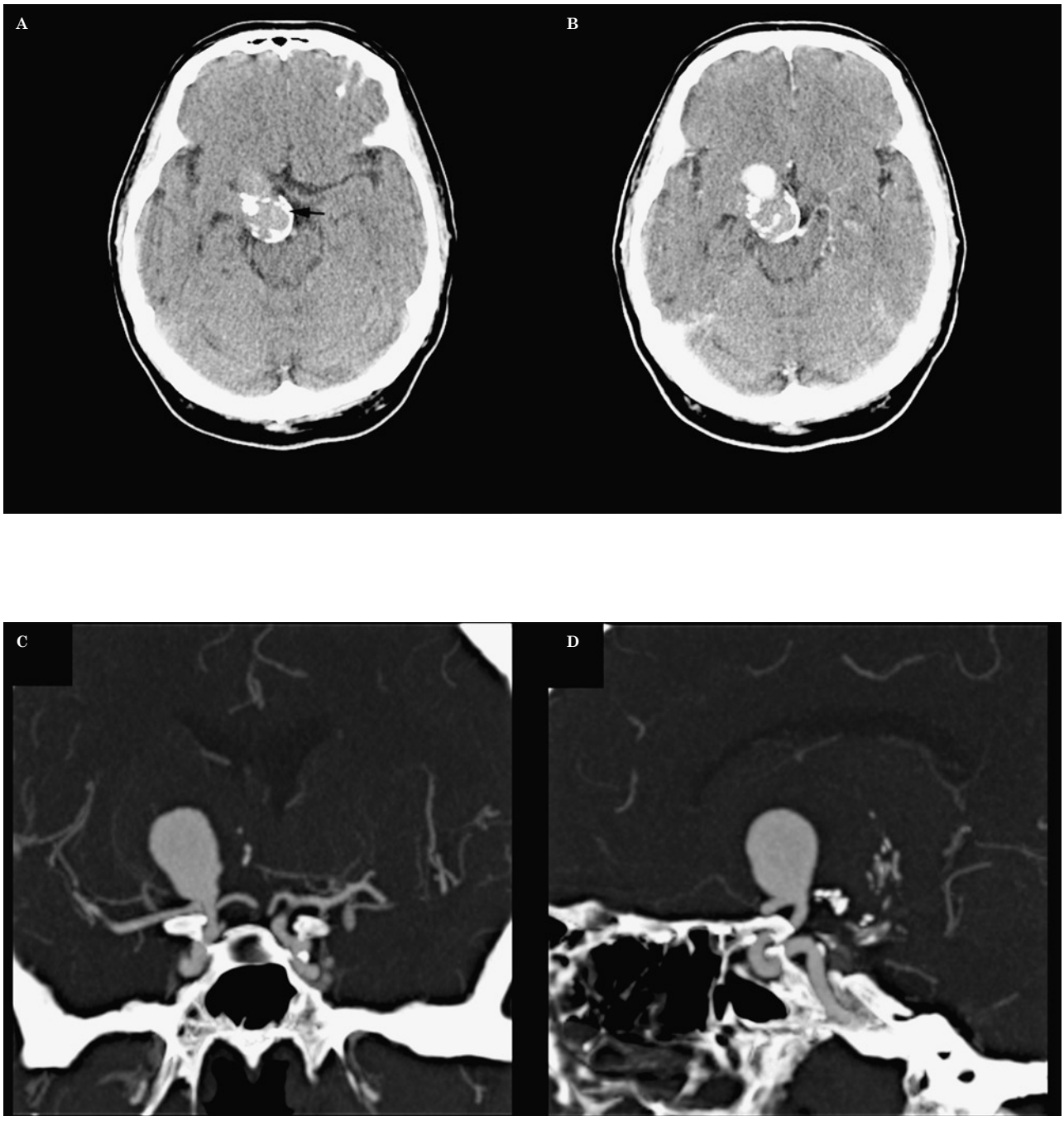

Figure 8 Aneurysm. A) Extensive curvilinear calcifications (arrow) are seen on a precontrast CT image in a patient with a saccular right middle cerebral artery aneurysm. Contrast is noted filling the aneurysm on the axial post contrast (B) and the coronal (C) and sagittal (D) maximum intensity projection (MIP) images.

plain radiography. Dystrophic intracranial calcifications are also seen in the watershed areas away from the AVM nidus due to ischemic brain tissue indicating vascular steal by the AVM [22].

Dural arteriovenous fistulas (AVFs) should be included in the differential diagnosis of intracranial calcification. Imaging studies may demonstrate bilateral and symmetrical subcortical calcification. This pattern of calcification

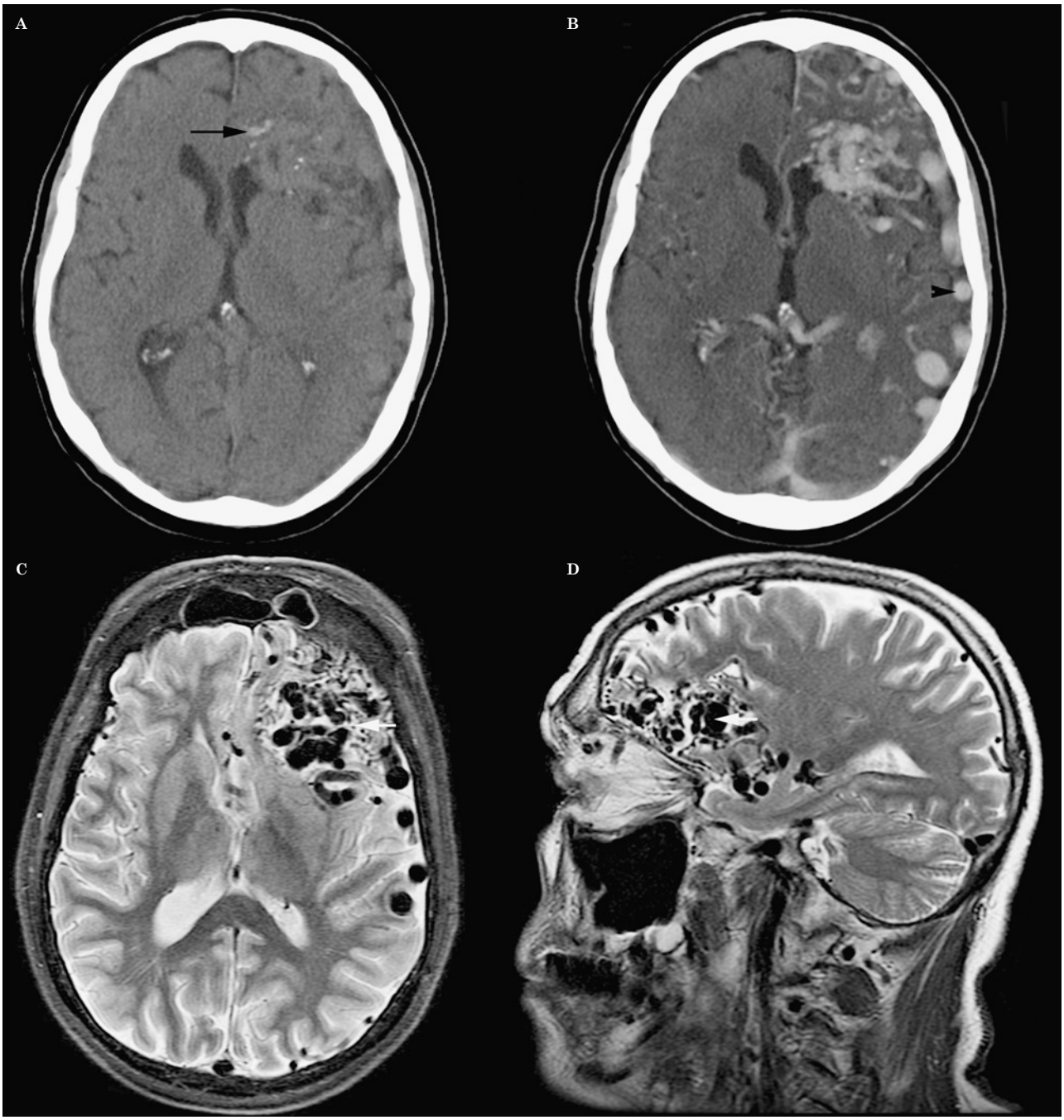

Figure 9 Arteriovenous malformation. A) Nonenhanced CT image demonstrates foci of coarse calcifications (arrow) in the left frontal lobe, associated with an underlying AVM. B) Post-contrast CT at the same level shows avid enhancement of the nidus, feeding and draining vessels. Note is made of prominent superficial cortical veins (arrowhead) overlying the left convexity. Axial (C) and sagittal (D) T2W images demonstrate a 'bag of worms' appearance (white arrows) of prominent flow voids associated with the AVM.

is a nonspecific imaging presentation and is seen more frequently in other conditions like Sturge-Weber syndrome, tuberous sclerosis, Fahr disease, and post chemo/radiotherapy change. However, unlike in the other conditions, no other foci of calcifications are found in AVF. The exact mechanism of the subcortical calcification is unknown but is proposed to be an 'arterial steal' phenomenon or persistent venous congestion [23]. Calcifications thus occur

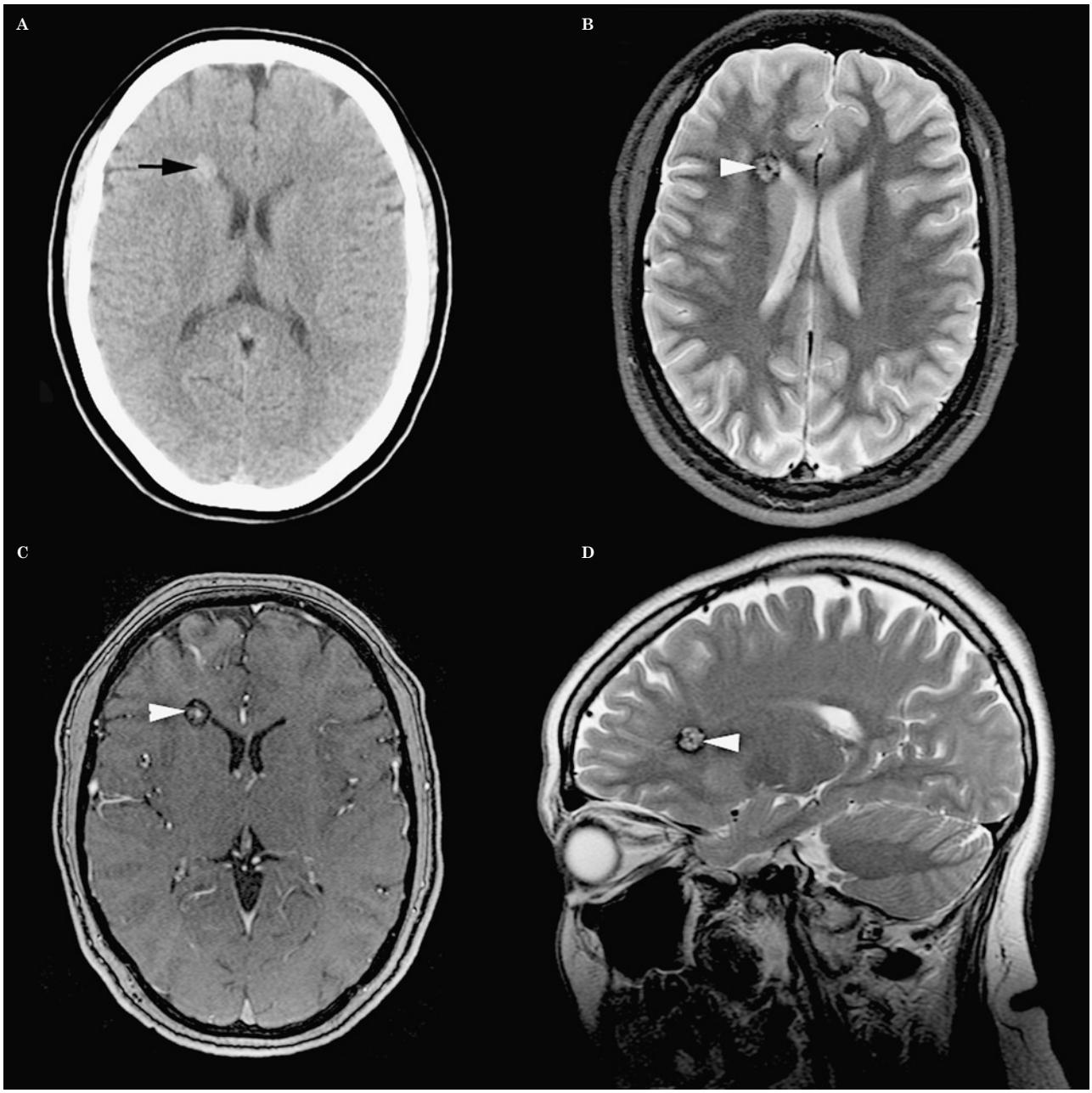

Figure 10 Cavernous angioma. A) Unenhanced CT demonstrates a well-defined hyperattenuating lesion (arrow) just lateral to the frontal horn of the right lateral ventricle. Areas of calcification and haemosiderin deposits, combined with the increased blood pool within the lesion, are responsible for the hyperattenuation on non-enhanced CT images. Axial T2W (B), axial T1W (C) and sagittal T2W images (D) demonstrate the characteristic 'popcorn ball' appearance (arrowheads) of mixed hyper-, and hypo- intense blood-containing locules.

in chronic hypoperfused brain parenchyma or secondary to dystrophic changes in the walls of congested veins. The cerebral subcortical white matter regions are located in the watershed areas of the arterial supply and therefore are more sensitive to hypoxia and ischaemia.

Computed tomography demonstrates calcifications in as many as 33% of cavernous angiomas. A well demarcated collection of rounded densities on CT, showing mild contrast enhancement and no significant mass effect, should suggest the diagnosis of a cavernous an-

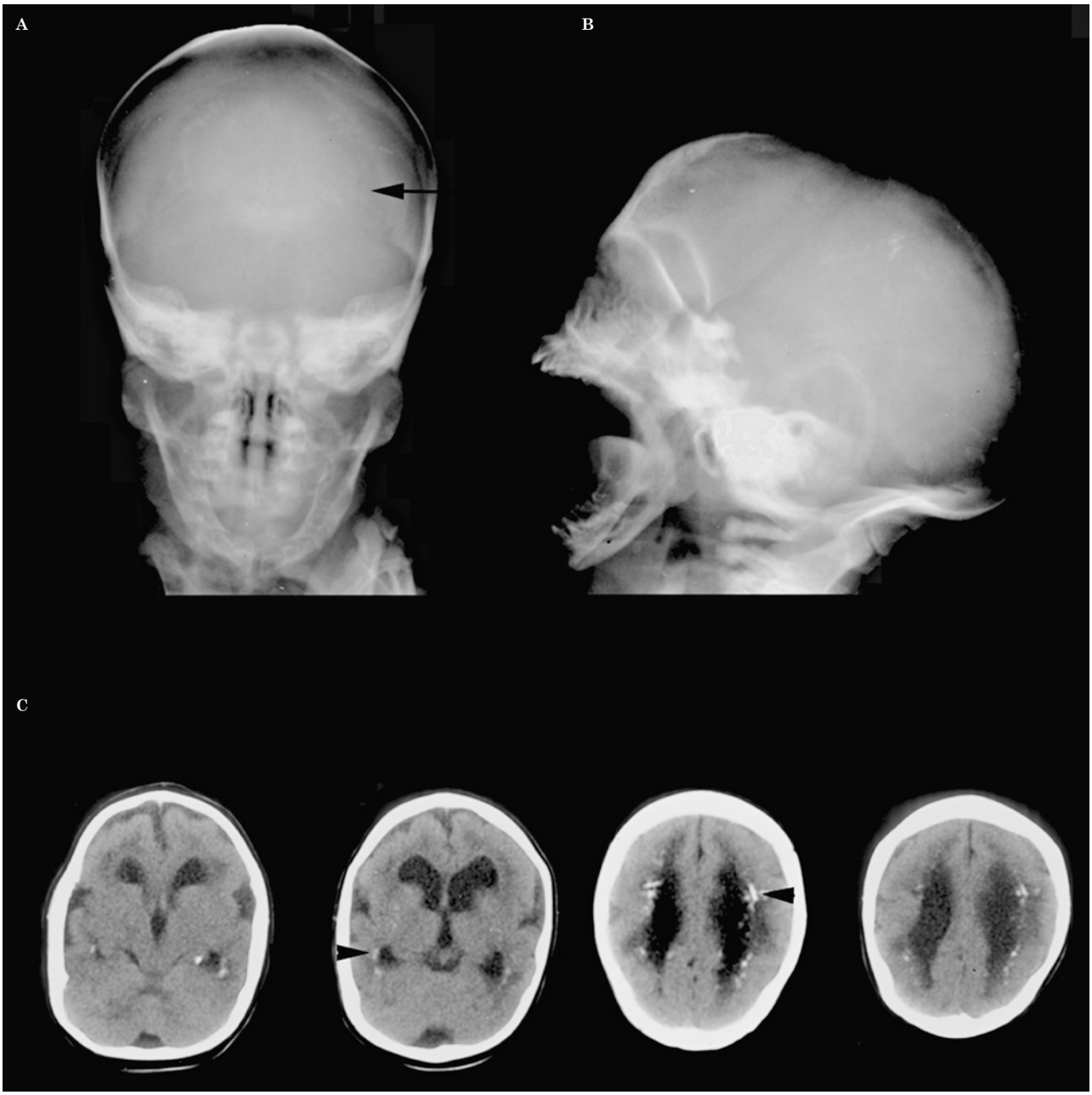

Figure 11 CMV infection. Frontal (A) and lateral (B) radiographs of an infant's skull reveal coarse calcifications (arrow) in the expected locations of the lateral ventricles. C) Non-contrast CT demonstrates the typical calcifications (arrowheads) deposited just beneath the ependyma of the ventricles.

gioma. Lesion size varies from a few millimetres to several centimetres. Areas of calcification and haemosiderin deposits in the walls of the fibrous septa, combined with the increased blood pool within the lesion, are responsible for hyperattenuation on non-enhanced CT images (Figure 10). The calcifications can also be identified on plain radiography in a minority of patients. MRI findings of parenchymal cavernous angiomas demonstrate typical, 'popcorn' like [24], smoothly circumscribed, well-delineated complex lesions. The core is formed by multiple foci

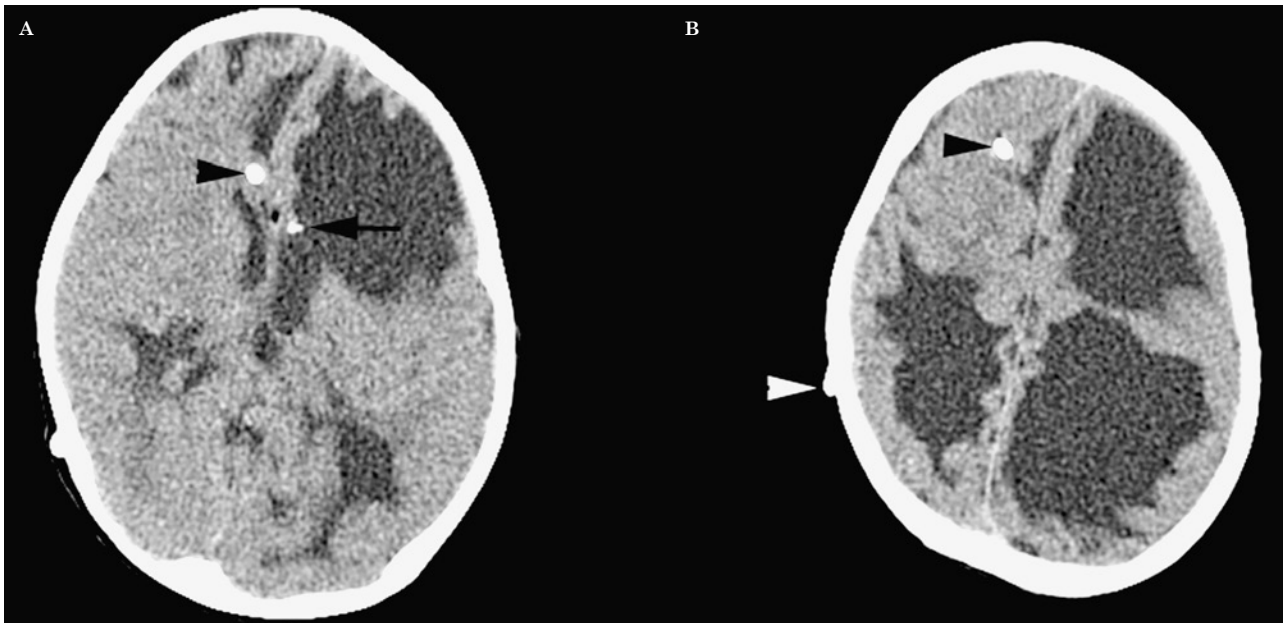

Figure 12 Congenital lymphocytic choriomeningitis. A) A subependymal focus of calcification (arrow) is noted in the medial wall of the left lateral ventricle. Porencephalic cysts and ventricular deformity (A,B) are often associated with this condition. Note the ventriculo-peritoneal shunt (arrowheads) to relieve hydrocephalus, often due to aqueductal obstruction. Head circumference was more than two standard deviations smaller than average (microcephaly).

Table 1 Basal ganglia calcifications.

	Basal ganglia calcifications	
A	Physiologic / Normal senescent	(most common)
B	Endocrine	Hypoparathyroidism Pseudohypoparathyroidism Pseudopseudohypoparathyroidism Hyperparathyroidism Hypothyroidism
C	Metabolic	Subacute necrotizing encephalomyelopathy (SNEM) Mitochondrial cytopathy Fahr disease
D	Ischaemic	Carbon monoxide intoxication Birth anoxia Cardiovascular event
E	Congenital / Developmental	Tuberous sclerosis Neurofibromatosis Trisomy 21 Familial idiopathic symmetric basal ganglia calcification Hastings-James syndrome Cockayne syndrome Lipoid proteinosis Methemoglobinopathy
F	Inflammatory / Infectious	Toxoplasmosis Cytomegalovirus Congenital rubella AIDS Cysticercosis Systemic lupus erythematosus Pertussis Coxsackie B virus Measles
G	Toxic	Lead intoxication Radiation therapy Chemotherapy Nephrotic syndrome Pantothenate kinase-associated neurodegeneration (PKAN)

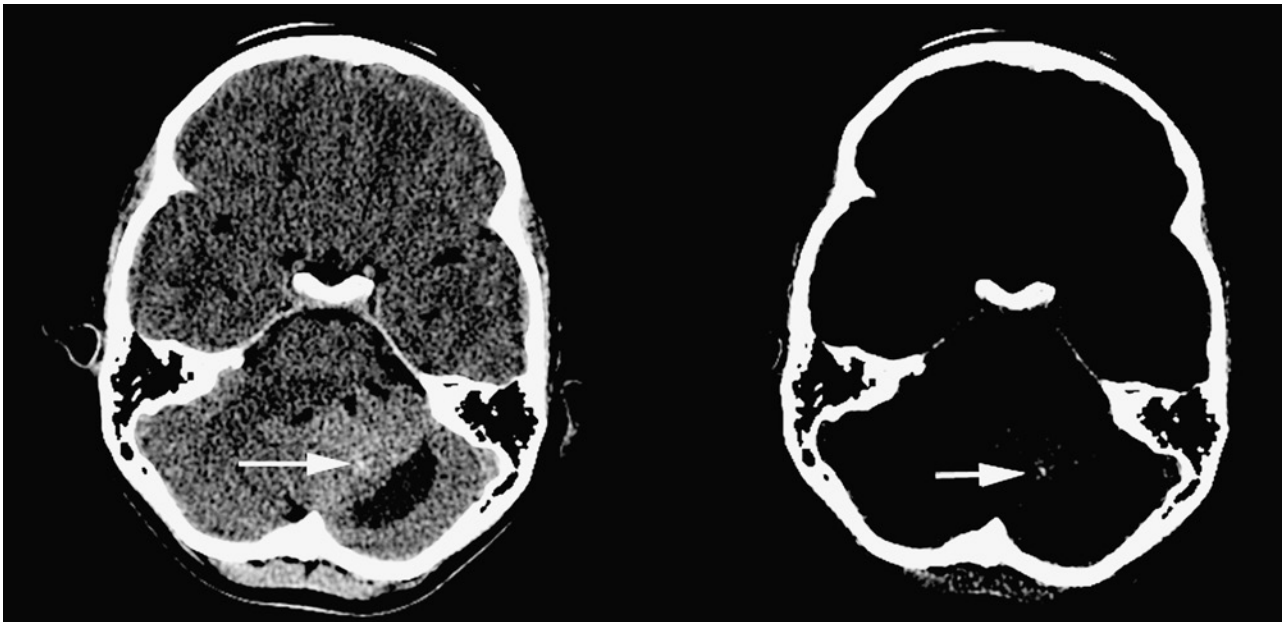

A B

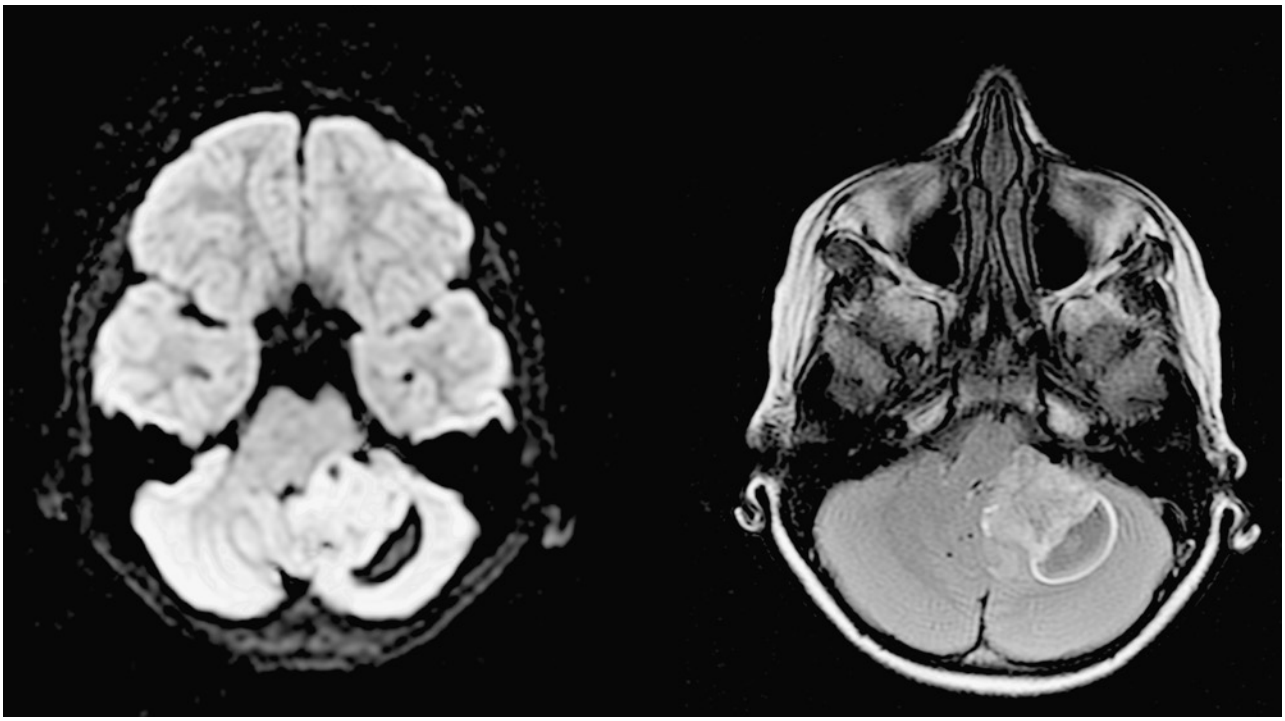

C D

Figure 13 Medulloblastoma (biopsy proven). A-D) Punctate calcifications are seen within a left cerebellar tumour on this nonenhanced CT through the posterior fossa (arrows). C) Diffusion-weighted image demonstrates typical restricted diffusion within the solid component of the tumour. D) Post contrast T1W MR image demonstrates avid enhancement of the tumour.

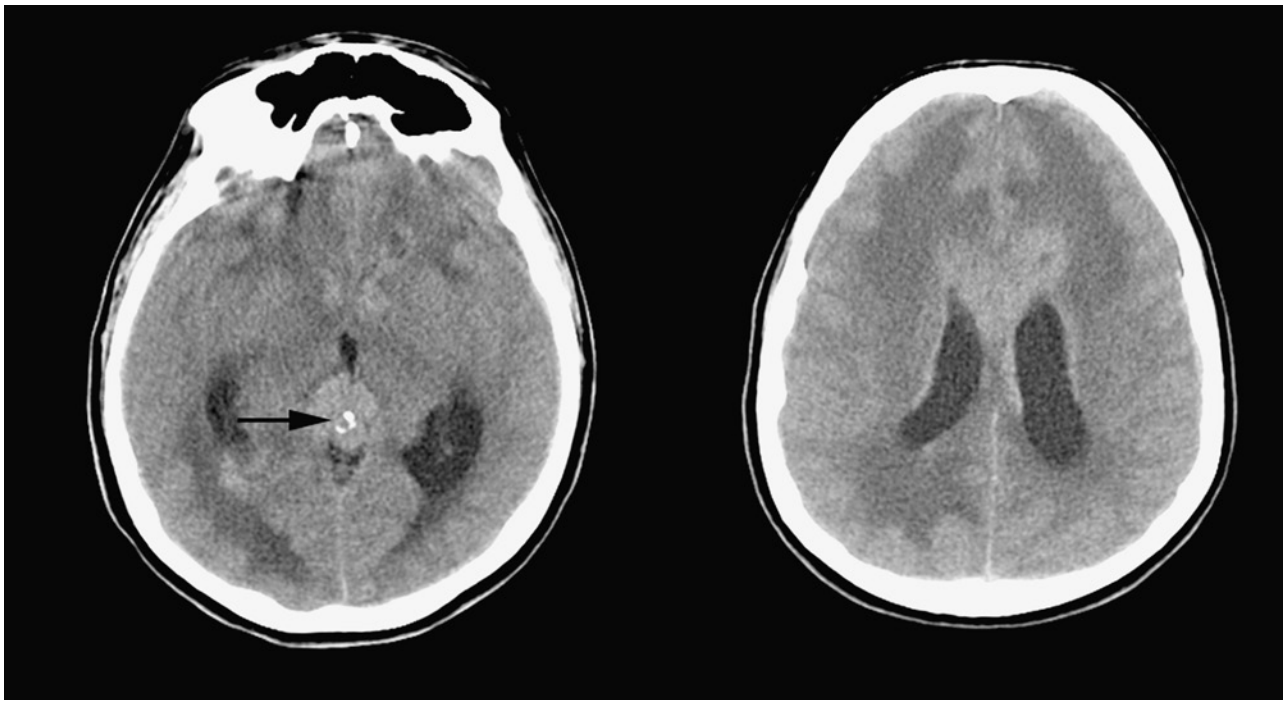

A B

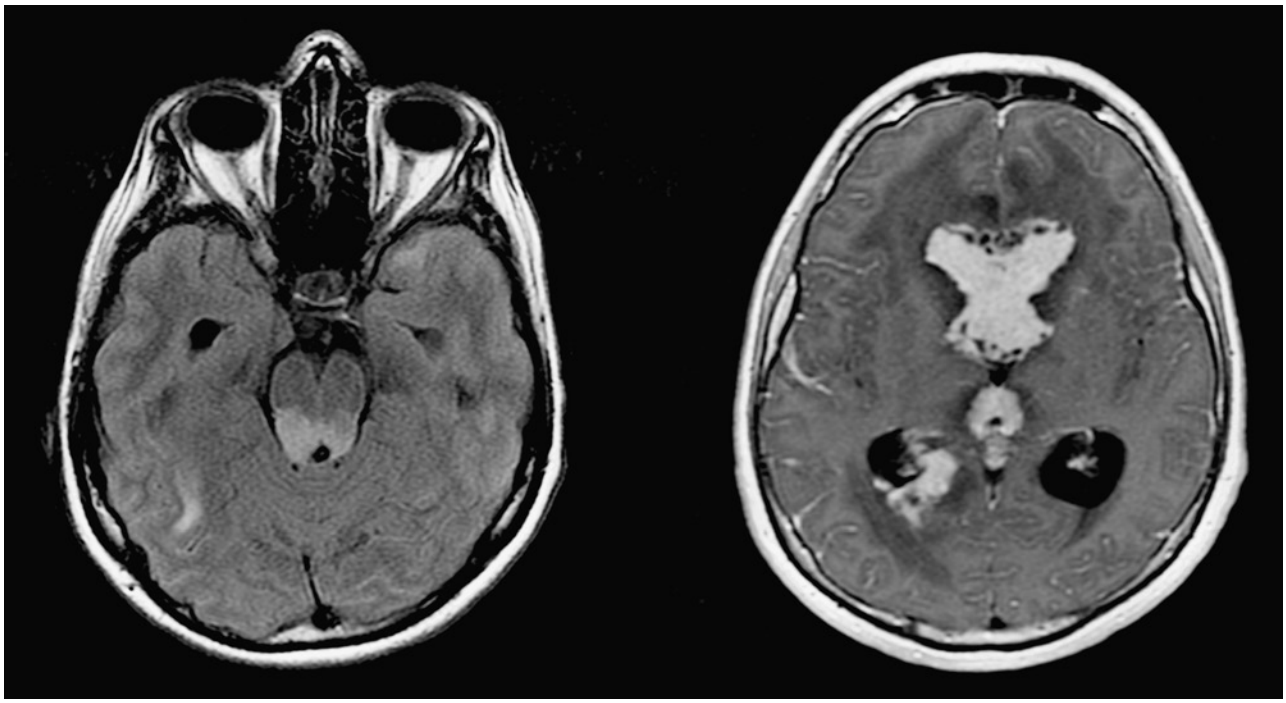

C D

Figure 14 Germinoma. A) Non-contrast CT shows a mass centred in the pineal region, which characteristically 'engulfs' the calcifications (arrow) within the pineal gland. The mass extends anteriorly as a midline mass between the lateral ventricles. Prominent vasogenic oedema is noted surrounding the tumour (A,B). Strong, homogenous enhancement is seen on enhanced T1W axial MR images (C,D).

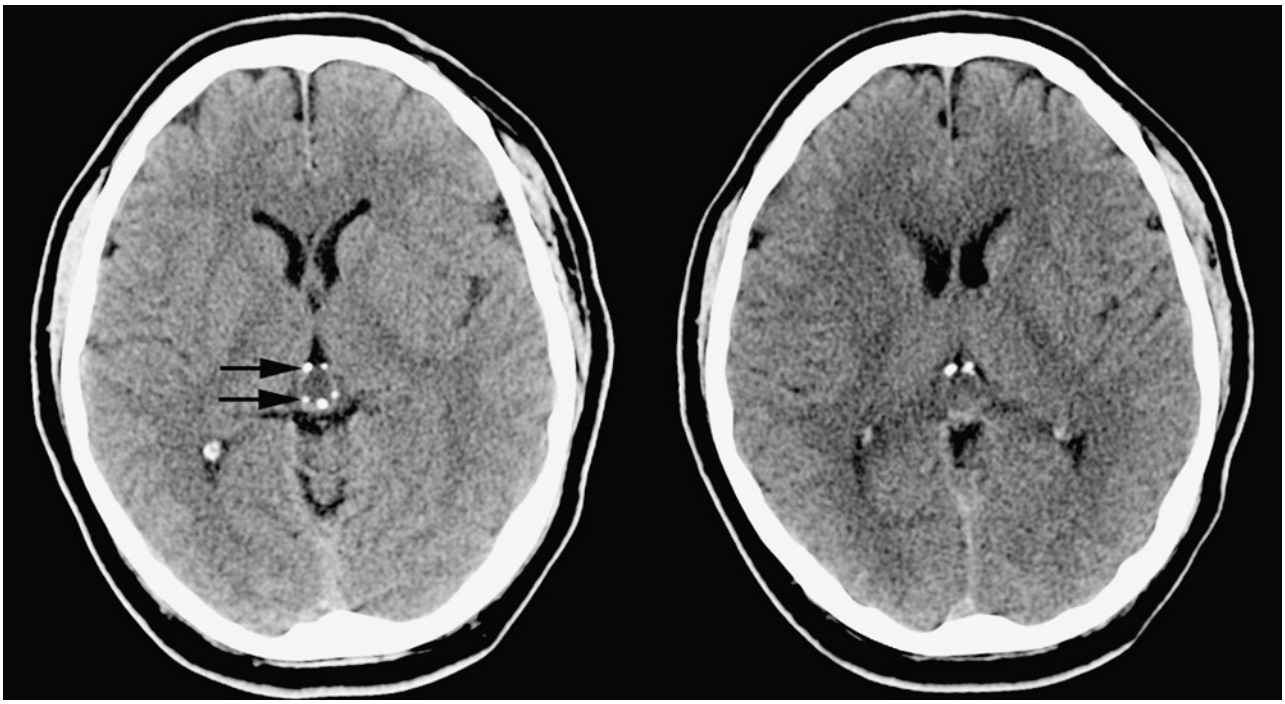

A B

Figure 15 Pineocytoma. Non-contrast CT images (A,B) demonstrate the typical 'exploded' peripheral calcifications (arrows) in this well circumscribed hypodense mass arising from the pineal region. There is no hydrocephalus. The patient had presented with Parinaud syndrome.

of mixed signal intensities, which represents haemorrhage in various stages of evolution.

Calcifications can be seen rarely in developmental venous anomalies (venous angioma) and capillary telangiectasias [25].

Amyloid angiopathy results in gyriform calcification and sclerotic changes in the medullary arteries [26].

Calcification of an ischemic infarction is rare [27] and is thought to occur months to years after the acute event. Brain calcification in such patients usually occurs in the setting of uraemia and hyperphosphatemia.

Infectious Calcifications

Both congenital and acquired CNS infections may be associated with intracranial calcifications. The most common *in utero* infections are those caused by TORCH agents including toxoplasmosis, rubella, Cytomegalovirus (CMV) and Herpes simplex virus (HSV).

Intracranial calcifications are the most common radiological abnormalities in CMV infection [28]. The calcifications are typically deposited just beneath the ependyma of the lateral ventricles [29] (Figure 11). However calcifications may also be seen throughout the brain parenchyma, and thus simulate toxoplasmosis. Congenital lymphocytic choriomeningitis produces a necrotizing ependymitis, which may eventually lead to aqueductal obstruction. The appearance on a non-enhanced CT may perfectly mimic CMV (Figure 12).

Toxoplasmosis is the commonest cause of intracranial calcifications in neonates. Nodular calcifications are seen in the periventricular regions and cerebral cortex. Curvilinear calcifications may also occur in the thalamus and basal ganglia. Interestingly, toxoplasma calcifications may resolve after treatment [30].

Scattered punctuate calcifications or extensive gyral calcifications occur in congenital HSV [31], whereas in congenital rubella calcifications are commonly located in the periventricular white matter, basal ganglia, and brain stem. Congenital HIV may show periventricular and cerebellar calcifications [32,33].

Cysticercosis [34,35], tuberculosis and cryptococcal infections represent the most common acquired CNS infections associated with calcifications. In tuberculosis, the parenchymal granulomata

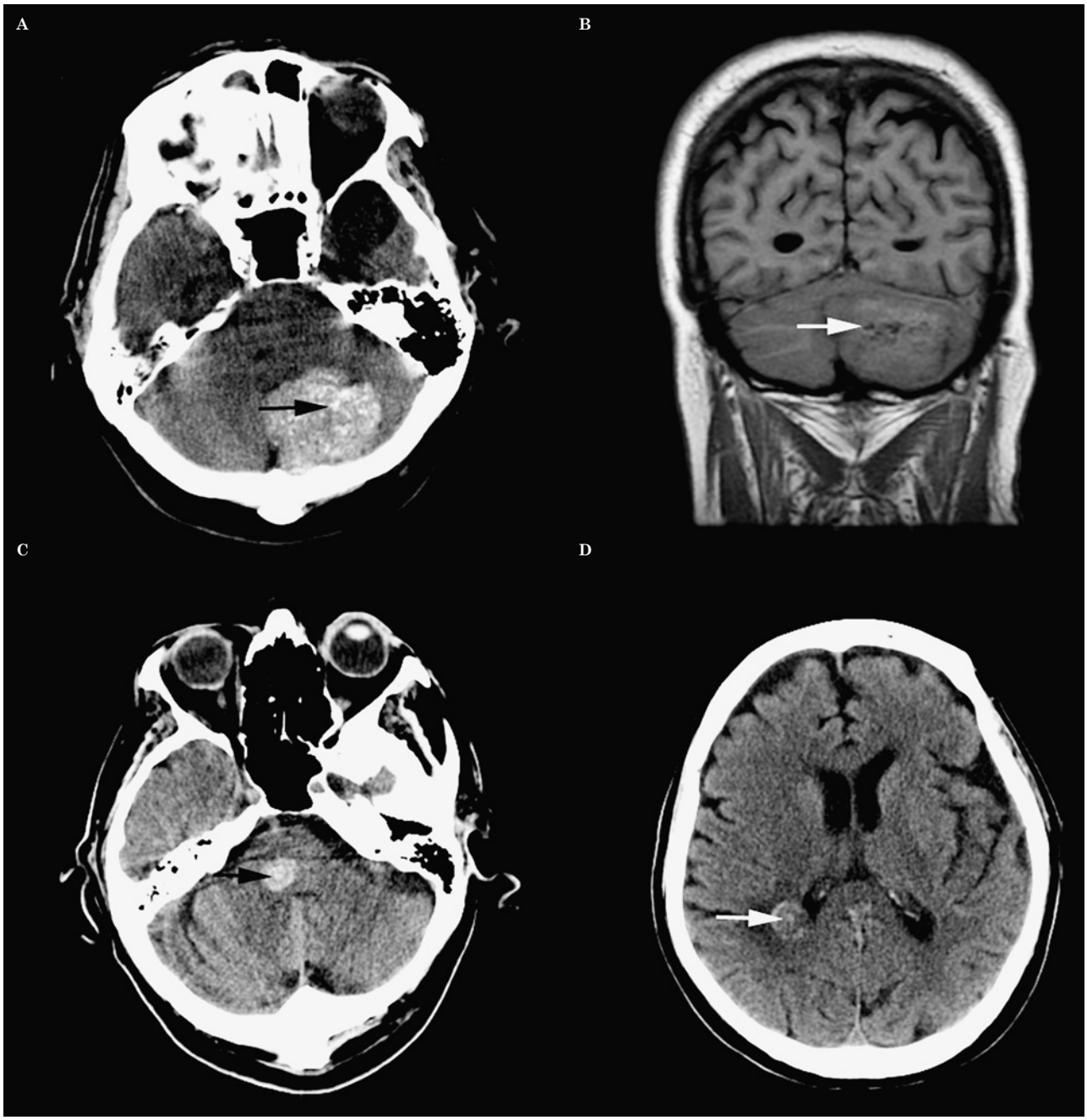

Figure 16 Metastasis. A) Noncontrast CT of the posterior fossa showing a large hyperdense intraaxial mass with foci of punctate calcifications (arrow). Coronal T1W MR (B) confirms the intraaxial location of the lesion and shows small foci of signal void (arrow) in keeping with calcifications. Histology revealed metastatic adenocarcinoma from a lung primary. Unenhanced CT images from a different patient with metastatic mucinous adenocarcinoma of the bowel, show a calcified lesion in the right cerebellar peduncle (C) and a further lesion more cranially (D). Vasogenic oedema surrounds the two lesions.

may calcify, giving the characteristic "target sign" representing a central nidus of calcification surrounded by a ring of enhancement[36]. Meningeal calcifications are much less common[6].

The granular phase of cysticercosis has a typical radiological appearance with a peripherally calcified cyst containing an eccentric calcified nodule. These occur both within the brain pa-

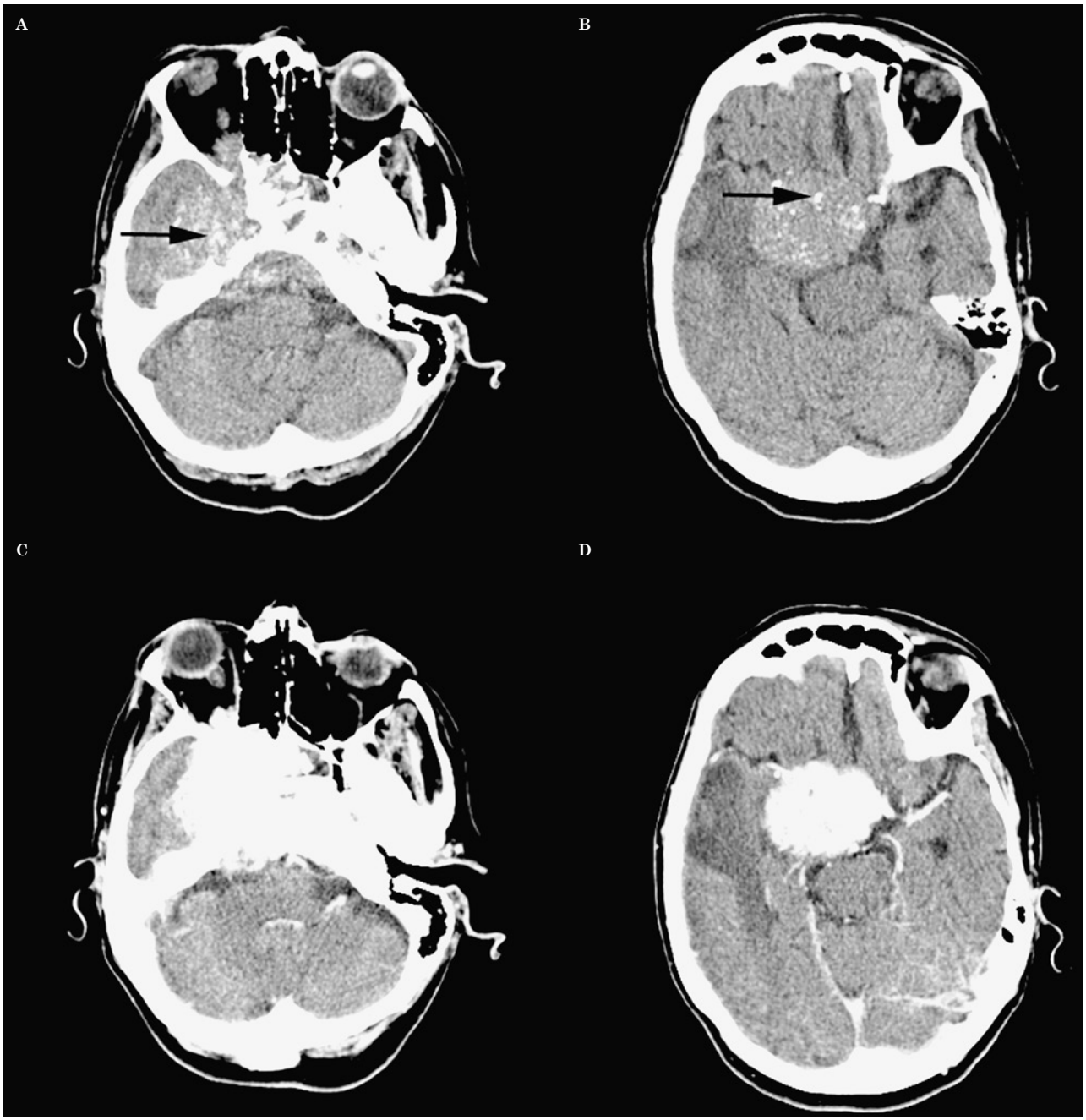

Figure 17 Meningioma. Noncontrast CT (A,B) reveals a large hyperdense lesion arising from the right sphenoid wing and extending into the suprasellar cistern. The mass contains coarse calcifications (arrows) and causes vasogenic oedema in the right temporal lobe. Avid enhancement is noted on the post-contrast images (C,D).

renchyma but also in the subarachnoid spaces.

Calcifications associated with cryptococcal infection can be seen in both the brain parenchyma and the leptomeninges [37,38], and most likely occur as a result of a protracted disease course.

Meningeal calcifications might also represent chronic sequelae of subdural and epidural empyemas [2].

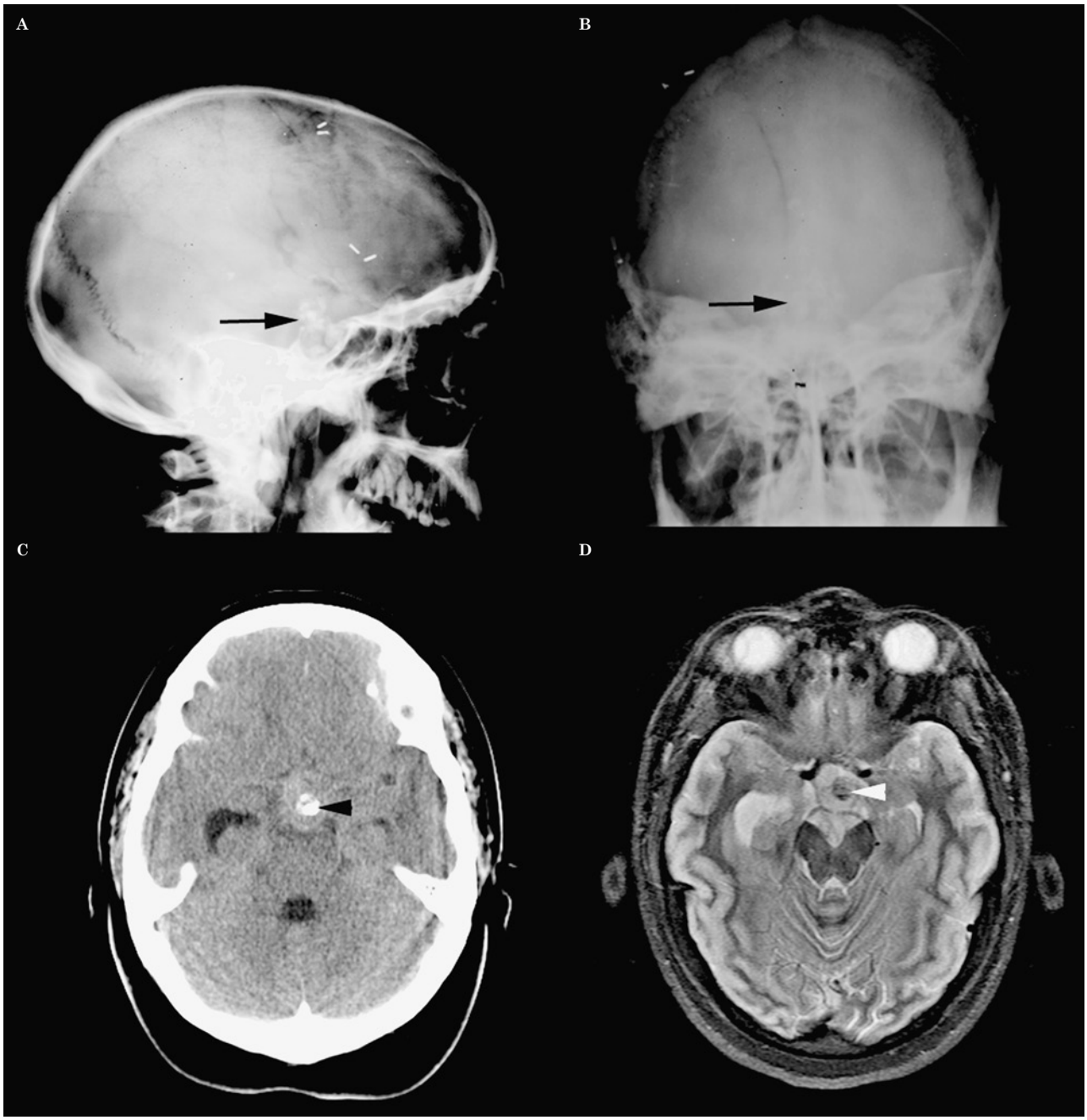

Figure 18 Craniopharyngoma. Lateral (A) and frontal (B) radiograph of the skull demonstrate a calcified mass (arrows) occupying an enlarged sella turcica and extending upwards into the suprasellar cistern. This represented local recurrence of a craniopharyngoma surgically treated years before. C) Non contrast CT shows coarse calcifications (arrowhead) within a suprasellar mass in a different patient. Axial T2W image at the same level demonstrates signal void from the calcifications (arrowhead) within the mass (D).

Calcifications in Inflammatory Disorders

Neurosarcoidosis has a predilection for the base of the brain and often involves the leptomeninges.

Calcified noncaseating granulomas may occur in the pituitary, pons, hypothalamus and the periventricular white matter [39]. Hypercalcaemia in sarcoidosis whether due to renal insufficiency or secondary hypoparathyroidism,

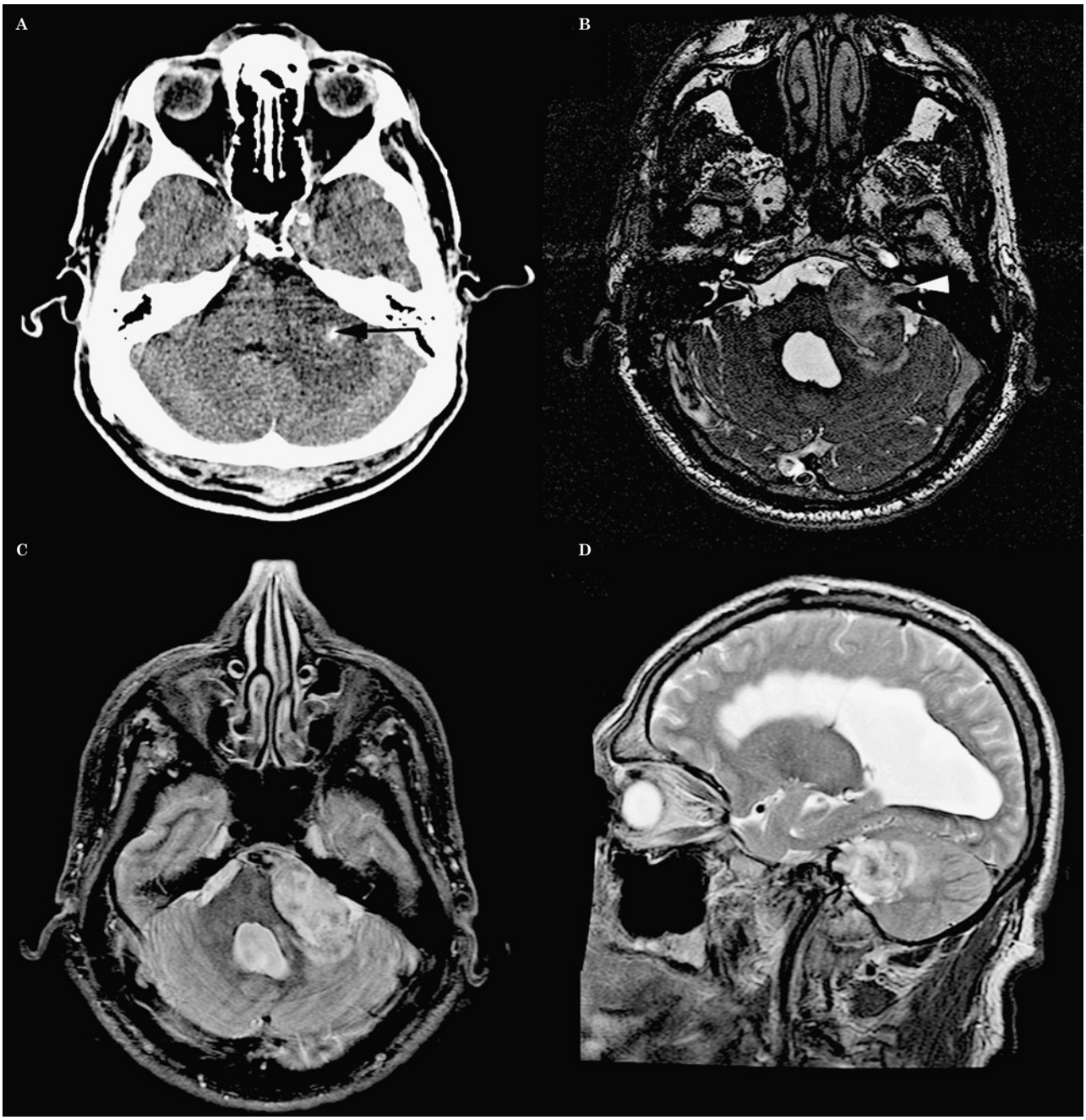

Figure 19 Vestibular schwannoma (biopsy proven). A) Unenhanced CT image shows a conspicuous calcification (arrow) within large cerebello-pontine angle mass. B) Axial FIESTA MR image reveals an intra-canalicular component (arrowhead) giving the appearance of an 'ice cream on cone' to the mass. Axial T2W (C) and sagittal (D) MR images confirm the location of the tumour to the CP angle, and also reveal a degree of hydrocephalus.

may also lead to ectopic or metastatic intracranial calcifications [40].

Cerebral lupus (CL) is a common cause of morbidity and mortality in patients with SLE. Cerebral calcifications have been described in the basal ganglia, thalamus, centrum semiovale, and cerebellum, with the globus pallidus representing the most commonly involved site [41].

There is no documented relationship between the degree of calcification and age of pa-

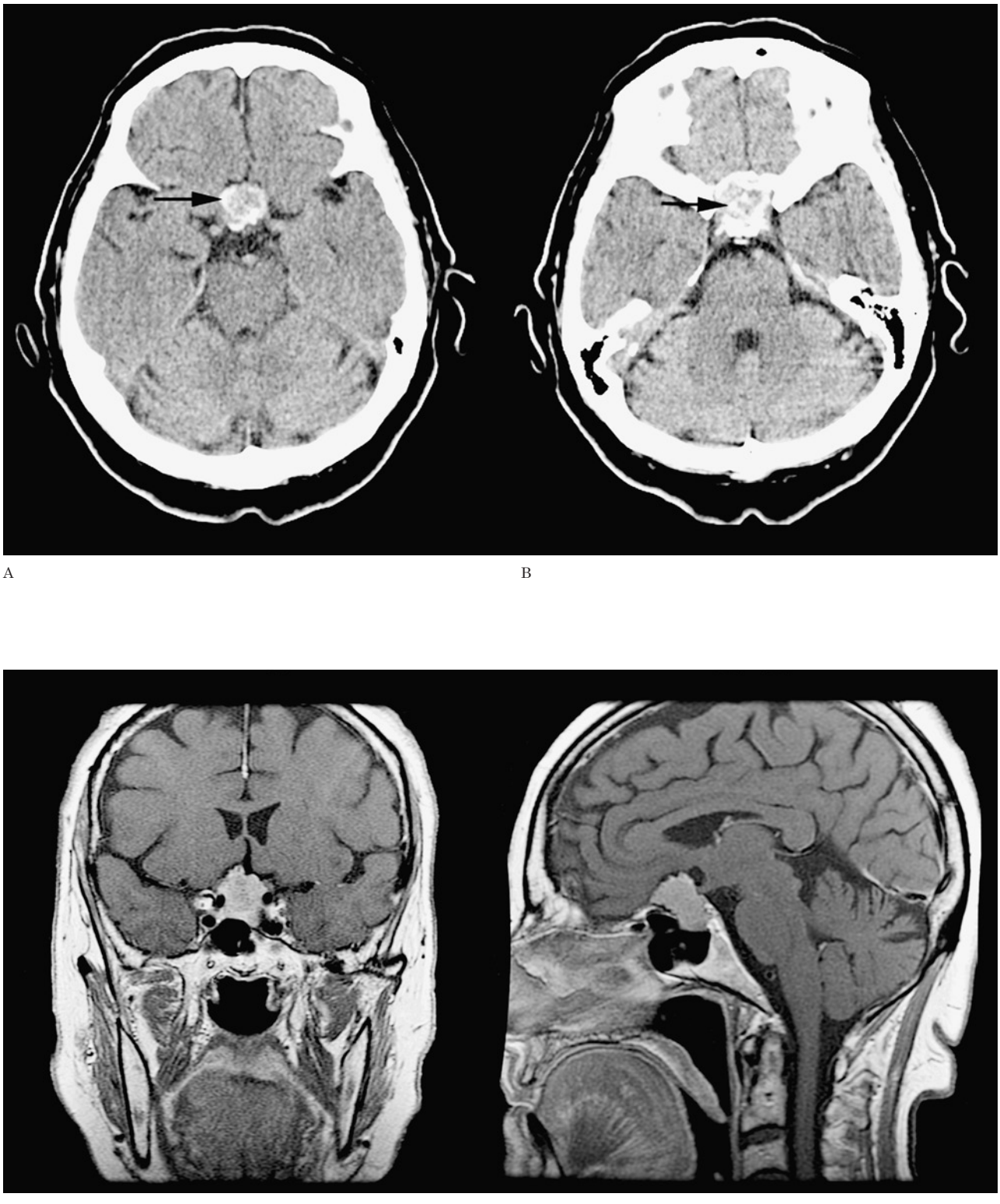

A B C D

Figure 20 Pituitary macroadenoma. Axial nonenhanced CT demonstrate a combined intra-/supra-sellar tumour with foci of macroscopic calcifications (arrow). Avid enhancement is seen on the coronal (A) and sagittal (D) contrast enhanced T1W images.

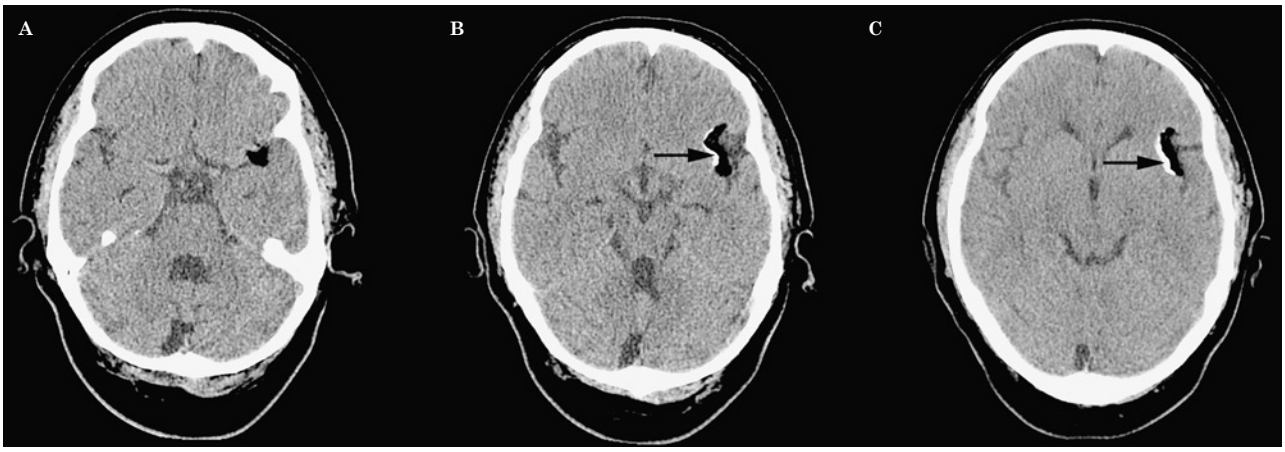

Figure 21 Lipoma. Axial noncontrast CT images reveal a well delineated lobulated extra-axial mass with fat attenuation (mean HU = –77) within the left sylvian fissure (A-C). 'Eggshell' calcification (arrows) is noted along its medial border.

tients or type of neurological presentation. The pathogenesis of cerebral calcification in CL remains unknown.

Neoplastic Calcifications

Calcifications represent an important tool for the radiological evaluation of brain tumours [42]. Along with the patient's age and tumour localisation, the presence and pattern of calcifications may help narrow the differential diagnosis, especially when the pattern is so characteristic as to be considered pathognomonic of a condition.

Although only 20% of astrocytomas exhibit calcification [2], they still represent the most common calcified intra-axial tumour, because of their high incidence. Up to 25% of pilocytic astrocytomas [43] demonstrate calcification; whereas high grade (WHO grades 3 and 4) astrocytomas only rarely calcify [44].

Ninety per cent of oligodendrogliomas calcify. Such calcifications are mostly associated with the intra tumoral vasculature; however they may extend into the surrounding parenchyma. Oligodendrogliomas are usually located in the frontal lobe and calcify in a nodular and clumped pattern [45,46]. A similar pattern of calcification is sometimes seen in relation to dysembryoplastic neuroepithelial tumours (DNETs) [47]. Medulloblastomas may also exhibit clump-like or nodular calcifications in approximately 20% of cases [48] (Figure 13).

Less common intra-axial tumours such as ganglioglioma may present as a cortically based cystic mass with a mural calcific nodule whereas a heterogeneous calcified mass in the pineal region in a young patient may suggest a germ cell tumour [6] (Figure 14). Calcification is seen in the majority of pineoblastomas and pineocytomas (60-80%) [2] (Figure 15). Some of the calcifications are native to the pineal gland itself giving the typical exploded appearance of calcifications in such tumours, whereas the more central calcifications are produced by the tumour itself.

Calcified metastases are rare, with the exception of osteogenic sarcoma, lung and breast primaries, and mucinous adenocarcinoma [49] (Figure 16). Calcifications in metastatic deposits may also develop as a sequel of radiotherapy or chemotherapy [3].

Calcifications occur in up to 69% of all meningiomas [43,50], and presents in several patterns including sand-like, sunburst, rim and globular calcifications distributed throughout the tumour mass [51] (Figure 17). Meningiomas also contain microscopic psammomatous calcifications, giving them an iso- to hyper-dense appearance to the adjacent brain parenchyma on non-enhanced CT.

Intraventricular meningiomas calcify in up to 50% of cases; choroid plexus tumours demonstrate typical punctuate calcifications in up to 25% of cases, while central neurocytomas [52] usually exhibit characteristic globular calcification. Intraventricular ependymomas [53] typically calcify, with a pattern ranging from punctate to nodular calcification.

The incidence of calcifications in craniopharyngomas (Figure 18) is associated with the underlying tumour histology [54]. Up to 90%

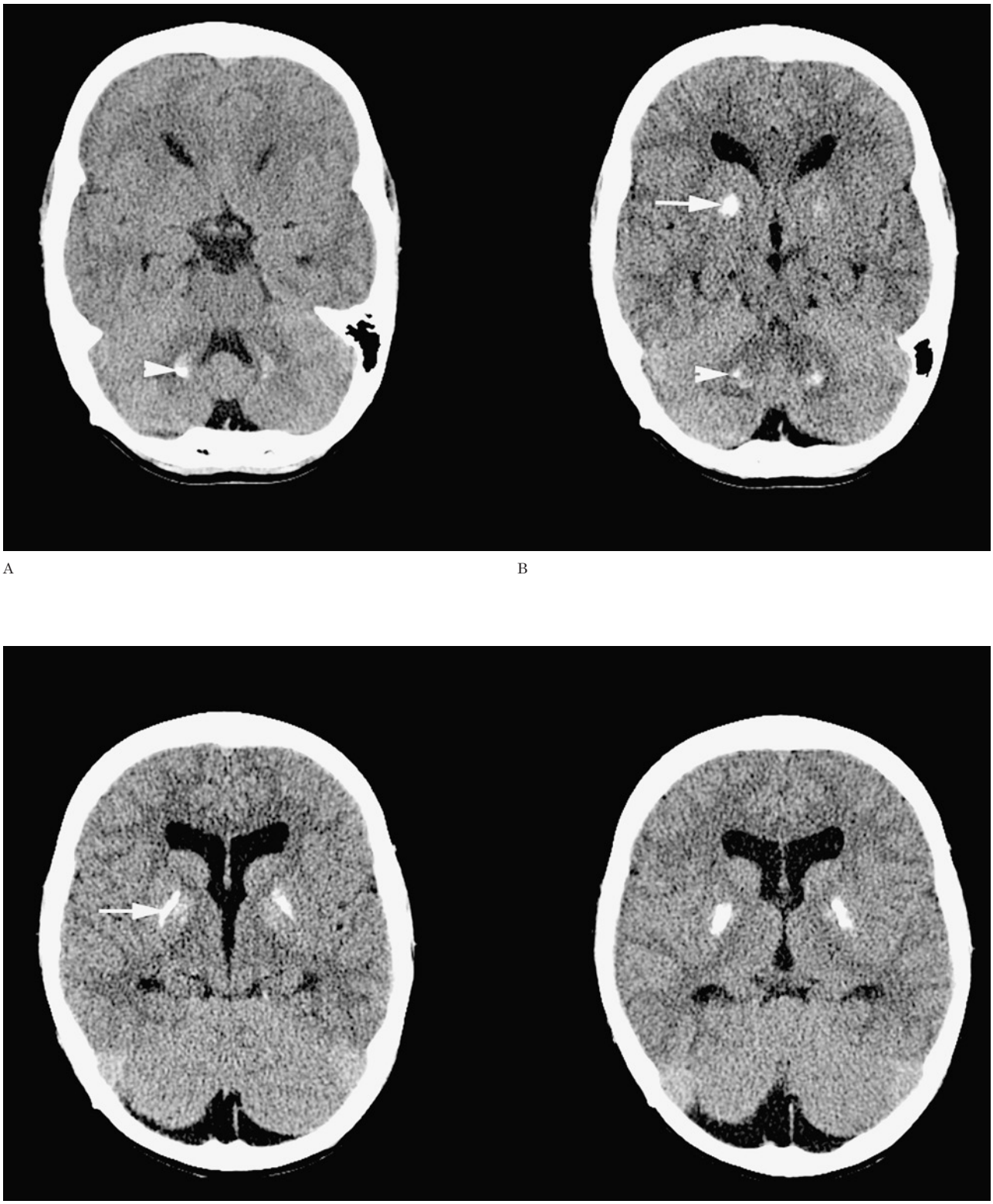

A B C D

Figure 22 Pseudohypoparathyroidism. A-D) Non enhanced CT images in a young patient with pseudohypoparathyroidism, demonstrates prominent bilateral basal ganglia (arrows) and cerebellar calcifications (arrowheads).

A B

Figure 23 Hyperparathyroidism. Dense calcifications of the falx cerebri and tentorium cerebelli (arrows) are seen on these non-contrast CT images (A,B). Further ectopic calcifications are seen in the corneal-scleral junction (arrowhead) and the subcutaneous tissues of the scalp.

of such tumours occurring in children demonstrate peripheral/rim calcification and calcification associated with the solid component of the tumour. In adults, craniopharyngomas are less likely to calcify. Calcifications are rarely seen in schwannomas (Figure 19), pituatory macroadenomas (Figure 20), dermoid and epidermoid tumors [55]. Eggshell calcification in lipomas [56] is due to calcification of their fibrous capsule (Figure 21); however calcifications can sometimes be seen centrally.

Endocrine Calcifications

Progression of parenchymal brain calcifications that appear similar to physiological calcifications should raise suspicion of an underlying metabolic disorder, especially if seen in young patients.

Pseudohypoparathyroidism [57] and to a lesser degree hypoparathyroidism [58] are the most common causes of pathological basal ganglia calcification. The globus pallidus is the most commonly affected part, but other sites include the cerebellum, sub cortical white matter, corona radiata and the thalamus (Figure 22).

Since adequate treatment of hypoparathyroidism may lead to marked clinical improvement, serum concentration of calcium, phosphorus, and parathyroid hormone (PTH) should be determined in individuals with basal ganglia calcifications to rule out underlying hypoparathyroidism [59].

Basal ganglia and subcortical calcifications also occur in patients with hyperparathyroidism (Figure 23), especially when associated with chronic renal failure (secondary hyperparathyroidism).

Hypervitaminosis D can also cause intracranial calcifications, especially in a basal ganglia distribution.

Conclusion

Radiologists should be familiar with the different patterns of calcifications and their appearances on different modalities. Although not always specific, the presence of intracranial calcification may be useful in narrowing down the differential diagnosis.

References

1 Kieffer SA, Gold LH. Intracranial physiologic calcifications. Semin Roentgenol. 1974; 2: 151-162.
2 Kiroglu Y, Calli C, Karabulut N, et al. Intracranial calcifications on CT. Diagn Interv Radiol. 2010; 16: 263-269.
3 Deepak S, Jayakumar B. Intracranial calcifications. J Assos Physicians India. 2005; 53: 948.
4 Zimmerman RA, Bilaniuk LT. Age-related incidence of pineal calcification detected by computed tomography. Radiology. 1982; 142: 659-662.
5 Koller WC, Klawans HL. Cerebellar calcification on computerized tomography. Ann Neurol. 1980; 7: 193-194.
6 Makariou E, Patsalides AD. Intracranial calcifications. App Radiol. 2009; 38: 11.
7 Wasenco JJ, Rosenbloom SA, Duchesneau PM, et al. The Sturge-Weber syndrome: comparison of MR and CT characteristic. Am J Neuroradiol. 1990; 1: 131-134.
8 Akpinar E. The tram-track sign: cortical calcifications. Radiology. 2004; 231: 515-516.
9 Kingsley DP, Kendall BE, Fitz CR. Tuberous sclerosis: A clinicoradiological evaluation of 110 cases with particular reference to atypical presentation. Neuroradiology. 1986; 28: 38-46.
10 Wilms G, Van Wijck E, Demaerel P, et al. Gyriform calcifications in tuberous sclerosis simulating the appearance of Sturge-Weber disease. Am J Neuroradiol. 1992; 13: 295-297.
11 Zatz LM. Atypical Choroid plexus calcifications associated with neurofibromatosis. Radiology. 1968; 91: 1135-1139.
12 Mayfrank L, Mohadjer M, Wullich B. Intracranial calcified deposits in neurofibromatosis type 2. A CT study of 11 cases. Neuroradiology.1990; 32: 33-37.
13 Vouge M, Pasquini U, Salvolini U. CT findings of atypical forms of phakomatosis. Neuroradiology. 1980; 20: 99-101.
14 Arts WF, Van Dongen KJ. Intracranial calcified deposits in neurofibromatosis. J Neurol Neurosurg Psychiatry. 1986; 49: 1317-1320.
15 Faria AV, Pereira IC, Nanni L. Computerized tomography findings in Fahr's syndrome. Arq Neuropsiquiatr. 2004; 62: 789-792.
16 El Maghraoui A, Birouk N, Zaim A, et al. Fahr syndrome and dysparathyroidism - 3 cases. Presse Med. 1995; 24: 1301-1304.
17 Lazăr M, Ion DA, Streinu-Cercel A, et al. Fahr's syndrome: diagnosis issues in patients with unknown family history of disease. Rom J Morphol Embryol. 2009; 50: 425-428.
18 Savy LE, Moseley IF. Intracranial arterial calcification and ectasia in visual failure. Br J Radiol. 1996; 69: 394-401.
19 de Weert TT, Cakir H, Rozie S, et al. Intracranial internal carotid artery calcifications: association with vascular risk factors and ischemic cerebrovascular disease. Am J Neuroradiol. 2009; 30: 177-184.
20 Chen XY, Lam WW, Ng HK, et al. The frequency and determinants of calcification in intracranial arteries in Chinese patients who underwent computed tomography examinations. Cerebrovasc Dis. 2006; 21: 91-97.
21 Tomandl BF, Köstner NC, Schempershofe M, et al. CT angiography of intracranial aneurysms: a focus on post processing. Radiographics. 2004; 3: 637-655.
22 Yu YL, Chiu EK, Woo E, et al. Dystrophic intracranial calcification: CT evidence of 'cerebral steal' from arteriovenous malformation. Neuroradiology. 1987; 29: 519-522.
23 Yang MS, Chen CC, Cheng YY, et al. Unilateral subcortical calcification: a manifestation of dural arteriovenous fistula. Am J Neuroradiol. 2005; 26: 1149-1151.
24 Metoki T, Mugikura S, Higano S, et al. Subcortical calcification on CT in dural arteriovenous fistula with cortical venous reflux. Am J Neuroradiol. 2006; 5: 1076-1078.
25 Fontaine S, de la Sayette V, Gianfelice D, et al. CT, MRI, and angiography of venous angiomas: A comparative study. Can Assoc Radiol J. 1987; 38: 259-263.
26 Terada S, Ishizu H, Tanabe Y, et al. Plaque-like structures and arteriosclerotic changes in "diffuse neurofibrillary tangles with calcification." Acta Neuropathol. 2001; 102: 597-603.
27 Wityk RJ, Lapeyrolerie D, Stein BD. Rapid brain calcification after ischemic stroke. Ann Intern Med. 1993; 119: 490-491.
28 Malinger G, Lev D, Zahalka N, et al. Fetal cytomegalovirus infection of the brain: the spectrum of sonographic findings. Am J Neuroradiol. 2003; 24: 28-32.
29 Ceola AF, Angtuaco TL. Cases of the Day: US Case of the Day. Radiographics. 1999, 19: 1385-1387.
30 Patel DV, Holfels EM, Vogel NP, et al. Resolution of intracranial calcifications in infants with treated congenital toxoplasmosis. Radiology. 1996; 199: 433-440.
31 Benator RM, Magill HL, Gerald B, et al. Herpes simplex encephalitis: CT findings in the neonate and young infant. Am J Neuroradiol. 1985; 6: 539-543.
32 Kauffman WM, Sivit CJ, Fitz CR, et al. CT and MR evaluation of intracranial involvement in pediatric HIV infection: A clinical-imaging correlation. Am J Neuroradiol. 1992; 13: 949-957.
33 Tovo PA, Gabiano C, Favro-Paris S, et al. Brain atrophy with intracranial calcification following congenital HIV infection. Acta Paediatr Scand. 1988; 77: 776-779.
34 Nash TE, Del Brutto OH, Butman JA, et al. Calcific neurocysticercosis and epileptogenesis. Neurology. 2004; 62: 1934-1938.
35 DeGiorgio CM, Medina MT, Durón R, et al. Neurocysticercosis. Epilepsy Curr. 2004; 4: 107-111.
36 Alkan A, Parlak M, Baysal T, et al. En-plaque tuberculomas of tentorium in a pregnant women: follow-up with MRI. Eur Radiol. 2003; 5: 1190-1193.
37 Caldemeyer KS, Mathews VP, Edwards-Brown MK, et al. Central nervous system cryptococcosis: parenchymal calcification and large gelatinous pseudocysts. Am J Neuroradiol. 1997; 18 (1): 107-109.
38 Caldemeyer KS, Mathews VP, Edwards-Brown MK, et al. Central nervous system cryptococcosis: Parenchymal calcification and large gelatinous pseudocysts. Am J Neuroradiol. 1997; 18: 107-109.
39 Magyari M, Frederiksen J. Neurosarcoidosis--different manifestations. Ugeskr Laeger. 2010; 172: 3344-3345.
40 Carson DR, Solomon FA Jr. Sarcoidosis: A Case with Extensive Metastatic Calcification, Renal Failure and Favorable Response to Steroid Therapy. Calif Med. 1962; 96: 114-118.
41 Raymond AA, Zariah AA, Samad SA, et al. Brain calcification in patients with cerebral lupus. Lupus.1996; 5: 123-128.
42 Becker H, Vonofakos D. Diagnostic significance of brain tumor calcifications in the computerized tomogram. Radiologe. 1983; 23: 459-462.
43 Ricci P. Imaging of adult brain tumors. Neuroimaging Clin N Am. 1999; 9: 651-669.
44 Teo JG, Goh KY, Ahuja A, et al. Intracranial vascular calcifications, glioblastoma multiforme, and lead poisoning. Am J Neuroradiol. 1997;18: 576-579. PubMed PMID: 9090426.
45 Vonofakos D, Marcu H, Hacker H. Oligodendrogliomas: CT patterns with emphasis on features indicating malignancy. J Comput Assist Tomogr. 1979; 3: 783-788.
46 Reiche W, Grunwald I, Hermann K, et al. Oligodendrogliomas. Acta Radiol. 2002; 43: 474-482.
47 Ostertun B, Wolf HK, Campos MG, et al. Dysembryoplastic neuroepithelial tumors: MR and CT evaluation. Am J Neuroradiol. 1996; 17: 419-430.
48 Meyers SP, Kemp SS, Tarr RW. MR imaging features of medulloblastomas. Am J Roentgenol. 1992; 158: 859-865.

49 Tomita T, Larsen MB. Calcified metastases to the brain in a child: Case report. Neurosurgery.1983; 13: 435-437.
50 Kizana E, Lee R, Young N, et al. A review of the radiological features of intracranial meningiomas. Australas Radiol. 1996; 40: 454-462.
51 Rees J, Lee SH, Smirniotopoulos JG. Primary brain tumors in adults. In: Lee SH. Rao KCVG, Zimmerman RA, eds. Cranial MRI and CT. 4th ed. New York: McGraw-Hill; 1999. p.261-341.
52 Yasargil MG, von Ammon K, von Deimling, et al. Central neurocytoma: Histopathological variants and therapeutic approaches. J Neurosurg. 1992; 76: 32-37.
53 Koeller KK, Sandberg GD; Armed Forces Institute of Pathology. From the archives of the AFIP. Cerebral intraventricular neoplasms: Radiologic pathologic correlation. Radiographics. 2002; 22: 1473-1505.
54 Tsuda M, Takahashi S, Higano S, et al. CT and MR imaging of craniopharyngioma. Eur Radiol. 1997; 7: 464-469.
55 Gao PY, Osborn AG, Smirniotopoulos JG, et al. Radiologic-pathologic correlation. Epidermoid tumor of the cerebellopontine angle. Am J Neuroradiol. 1992; 13: 863-872.
56 Dean B, Drayer BP, Beresini DC, et al. MR imaging of pericallosal lipoma. Am J Neuroradiol. 1988; 9: 929-931.
57 Fujita T. Mechanism of intracerebral calcification in hypoparathyroidism. Clin Calcium. 2004; 14: 55-57.
58 You JS, Kim HJ, Chung SP, et al. Intracranial bilateral symmetric calcification in hypoparathyroidism. Emerg Med J. 2008; 3: 162.
59 Basak R. A Case Report of Basal Ganglia Calcification - A Rare Finding of Hypoparathyroidism OMJ. 2009; 24: 220-222; doi:10.5001/omj.2009.43.

Reuben Grech, MD, MRCS (Ed), FRCR (UK), FFR RCSI (Ire) EDiR
Waterford Regional Hospital
Waterford, Ireland
E-mail: reubengrech@yahoo.com